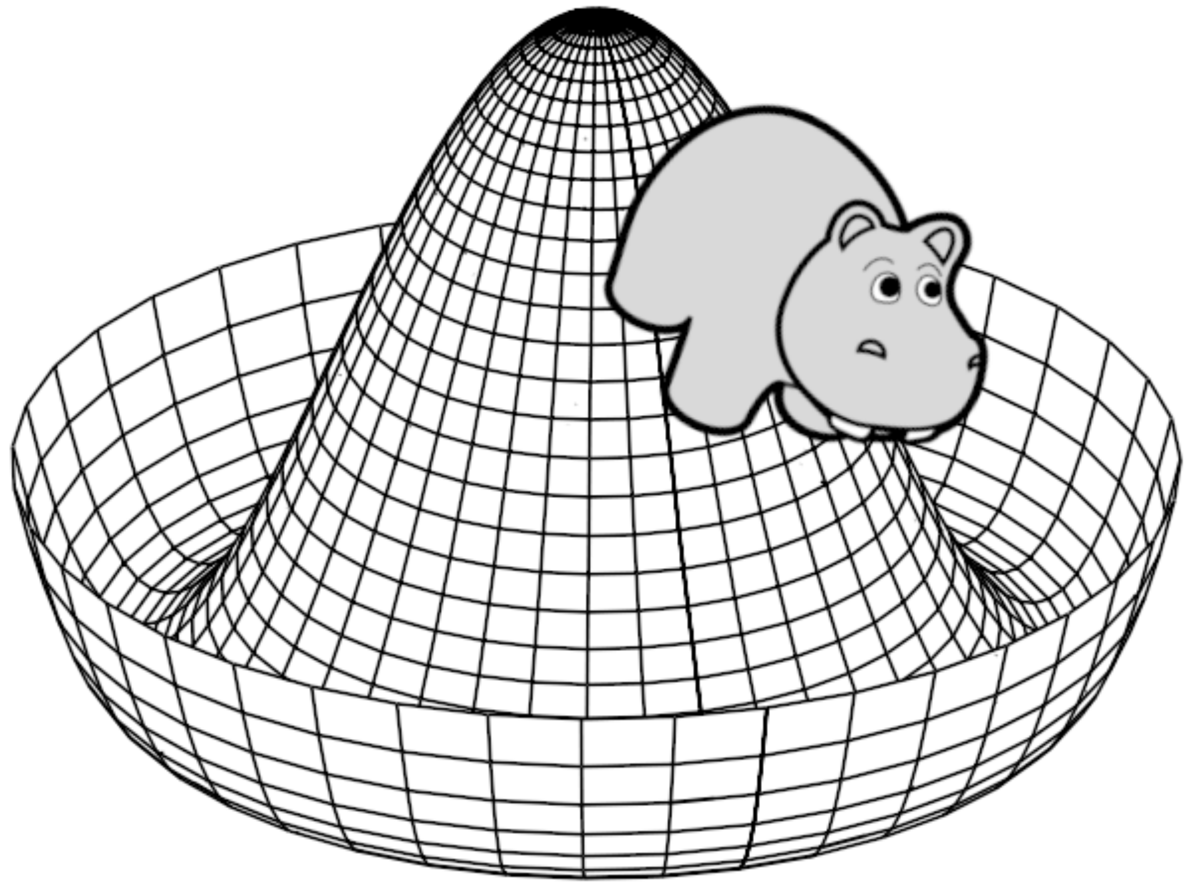

Overview of ATLAS HH results in Run 2 and Run 3 plans

Christina Dimitriadi, Arnaud Ferrari, Philipp Rincke

6 December 2023

UPPSALA UNIVERSITET

UNIVERSITÄT BONN

CONF note for Higgs 2023

ATLAS Note

Report number	ATLAS-CONF-2023-071
Title	**Search for the non-resonant production of Higgs boson pairs via gluon fusion and vector-boson fusion in the $b\bar{b}\tau^+\tau^-$ final state in proton-proton collisions at $\sqrt{s}$ = 13 TeV with the ATLAS detector**
Corporate Author(s)	The ATLAS collaboration
Collaboration	ATLAS Collaboration
Imprint	26 Nov 2023. - 28 p.
Note	All figures including auxiliary figures are available at https://atlas.web.cern.ch/Atlas/GROUPS/PHYSICS/CONFNOTES/ATLAS-CONF-2023-071
In:	Higgs 2023, Beijing, Cn, 27 Nov - 2 Dec 2023
Subject category	Particle Physics - Experiment
Accelerator/Facility, Experiment	CERN LHC ; ATLAS
Abstract	A search for the non-resonant production of Higgs boson pairs in the $HH \to b\bar{b}\tau^+\tau^-$ channel is performed using 140 fb^{-1} of proton-proton collisions at a centre-of-mass energy of 13 TeV recorded by the ATLAS detector at the CERN Large Hadron Collider. The analysis strategy is optimised to probe anomalous values of the Higgs boson self-coupling modifier κ_λ and of the quartic $HHVV$ $(V = W, Z)$ coupling modifier κ_{2V}. No significant excess above the expected background from Standard Model processes is observed. An observed (expected) upper limit $\mu_{HH} < 5.9(3.1)$ is set at 95\% confidence-level on the Higgs boson pair production cross-section normalised to its Standard Model prediction. The coupling modifiers are constrained to an observed (expected) 95\% confidence interval of $-3.2 < \kappa_\lambda < 9.1$ $(-2.5 < \kappa_\lambda < 9.2)$ and $-0.4 < \kappa_{2V} < 2.6$ $(-0.2 < \kappa_{2V} < 2.4)$, assuming all other Higgs boson couplings are fixed to the Standard Model prediction. The results are also interpreted in the context of effective field theories.

CDS entry

- Legacy Run 2 HH→bbττ search
  - Signal strength limits
  - Constraints on anomalous couplings
  - EFT interpretation
- Journal submission to follow soon, once full EFT is included
- Previous full Run 2 search (not optimised for non-resonant) [JHEP 07 (2023) 040]

The HH→bbττ search

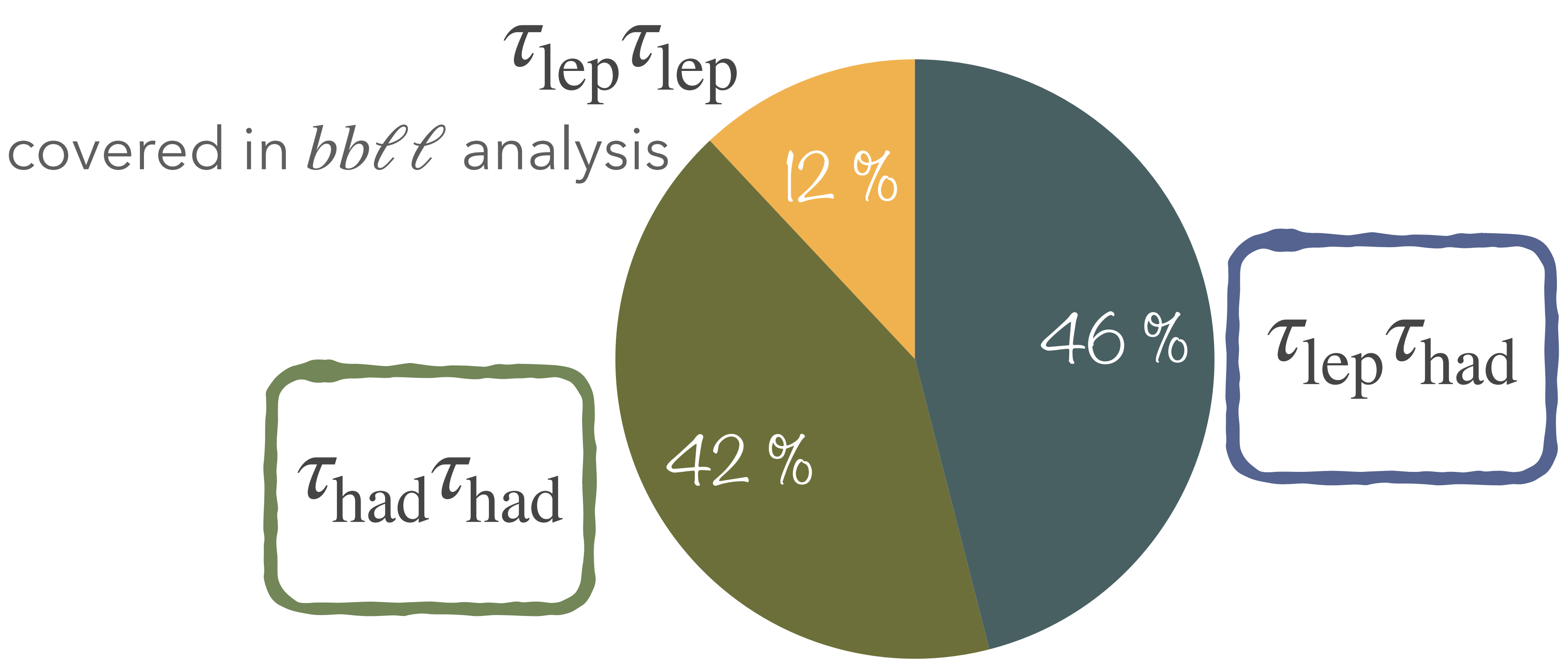

- Two channels split by di-tau decay mode, $\tau_{had}\tau_{had}$ and $\tau_{lep}\tau_{had}$ and further categorised by triggers:

$\tau_{had}\tau_{had}$	+	$\tau_{lep}\tau_{had}$ SLT	+	$\tau_{lep}\tau_{had}$ LTT
single- and di-τ_{had} triggers		single-ℓ triggers		$\ell + \tau_{had}$ triggers

x 3 signal regions based on production mode and m_{HH} split

ggF low-m_{HH} + ggF high-m_{HH} + VBF

+ 1 control region

m_{ll} ($Z \rightarrow ee/\mu\mu$ + HF) CR

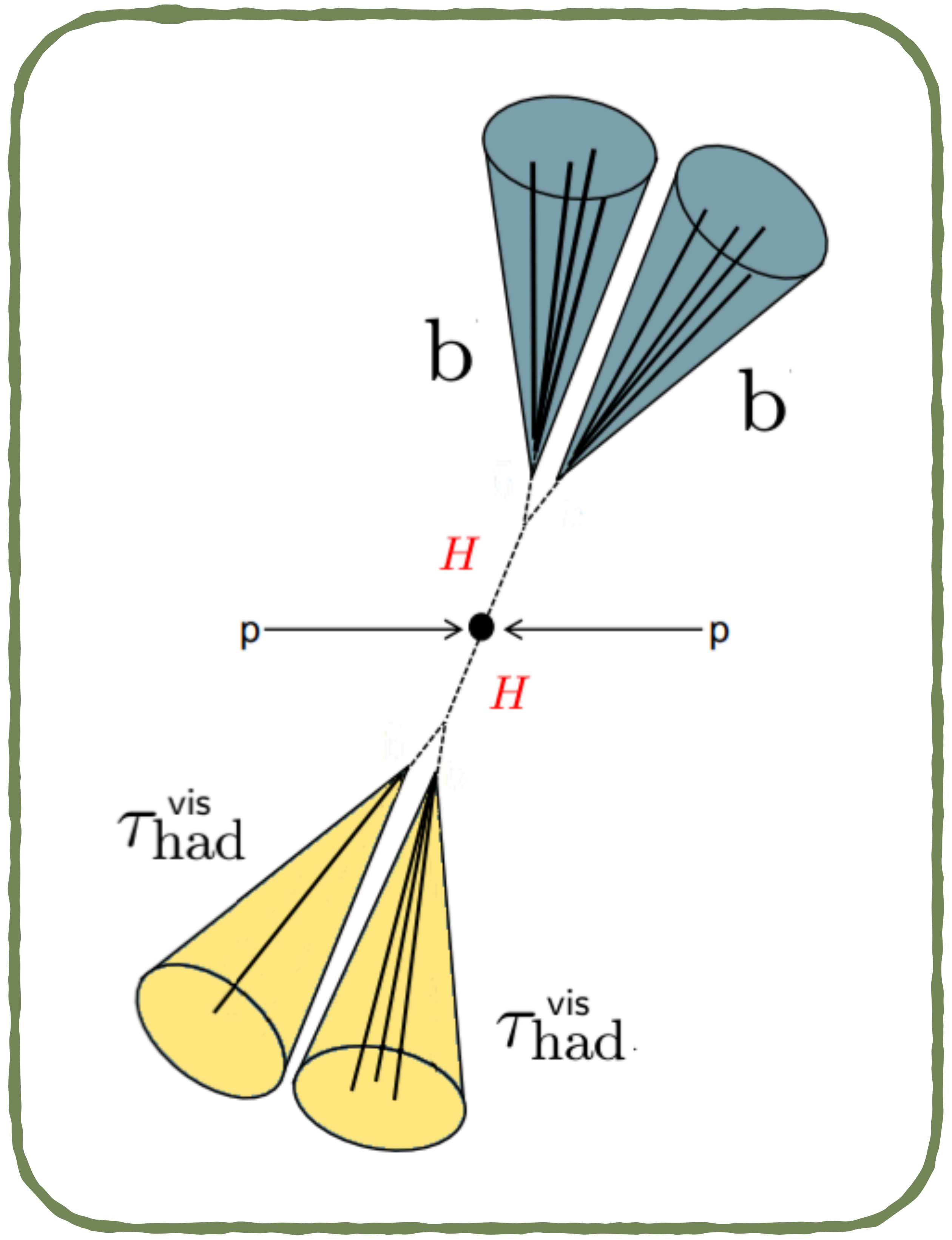

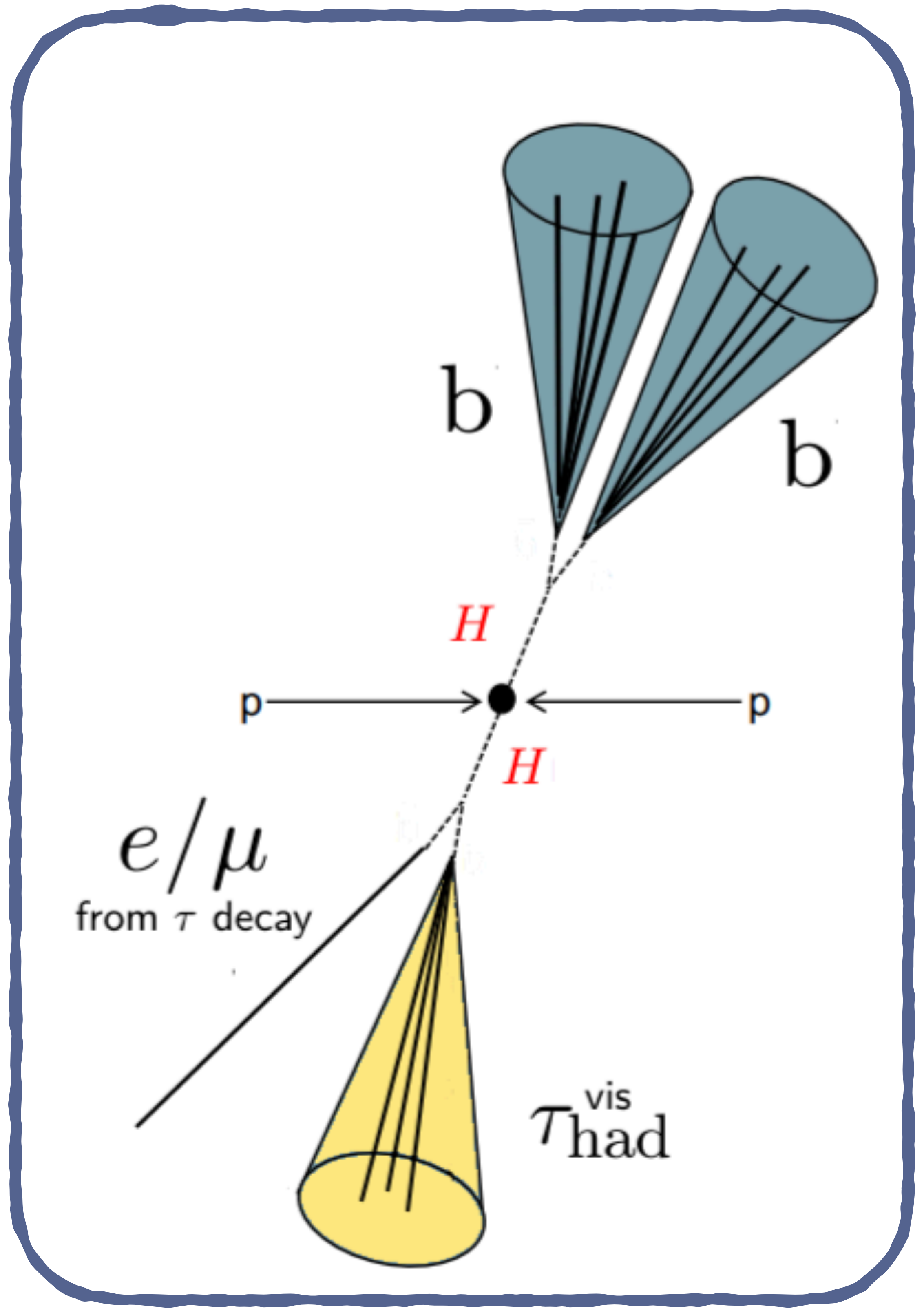

- Main backgrounds:
  - true taus from $t\bar{t}$ and $Z \rightarrow \tau\tau$ + HF
  - fake taus from multi-jet and $t\bar{t}$ processes

Analysis overview (now and then)

- Same trigger strategy, object reconstruction & identification and event selection as previous Run 2 analysis

Previous analysis

Inclusive SR for ggF and VBF → **Dedicated ggF** (high-m_{HH}, low-m_{HH}) **and VBF regions:** *Simultaneous constraints possible*

BDT in had-had, NN in lep-had → **Fully harmonized MVA strategy:** *Optimised BDTs in both channels as fit discriminant and for ggF/VBF classification*

This analysis

New background MC samples: *Dilepton ttbar, Z+jets Sherpa 2.2.11 & aMC@NLO FxFx, single top → less MC stat uncertainty, easier modelling*

Optimised binning

EFT interpretation of results

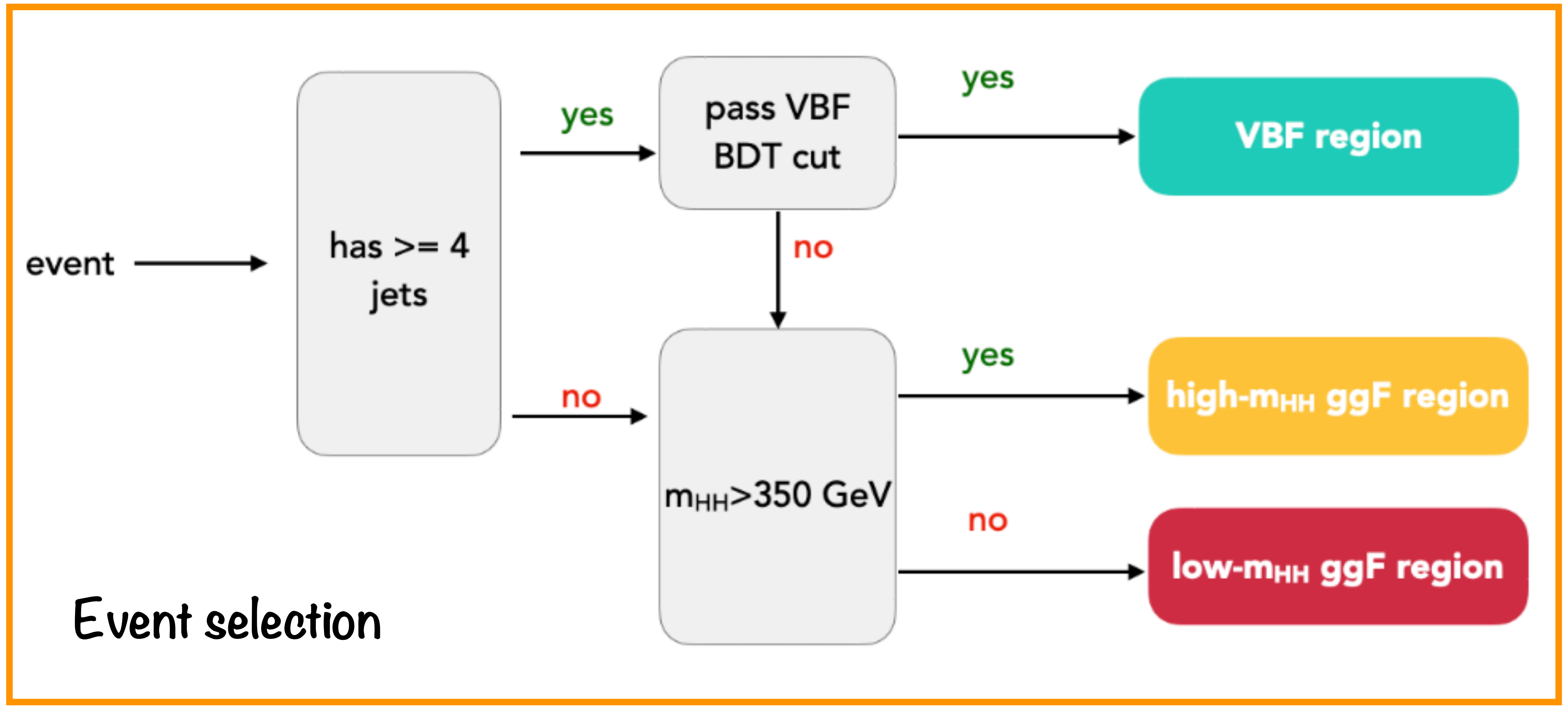

ggF HH vs. VBF HH categorisation

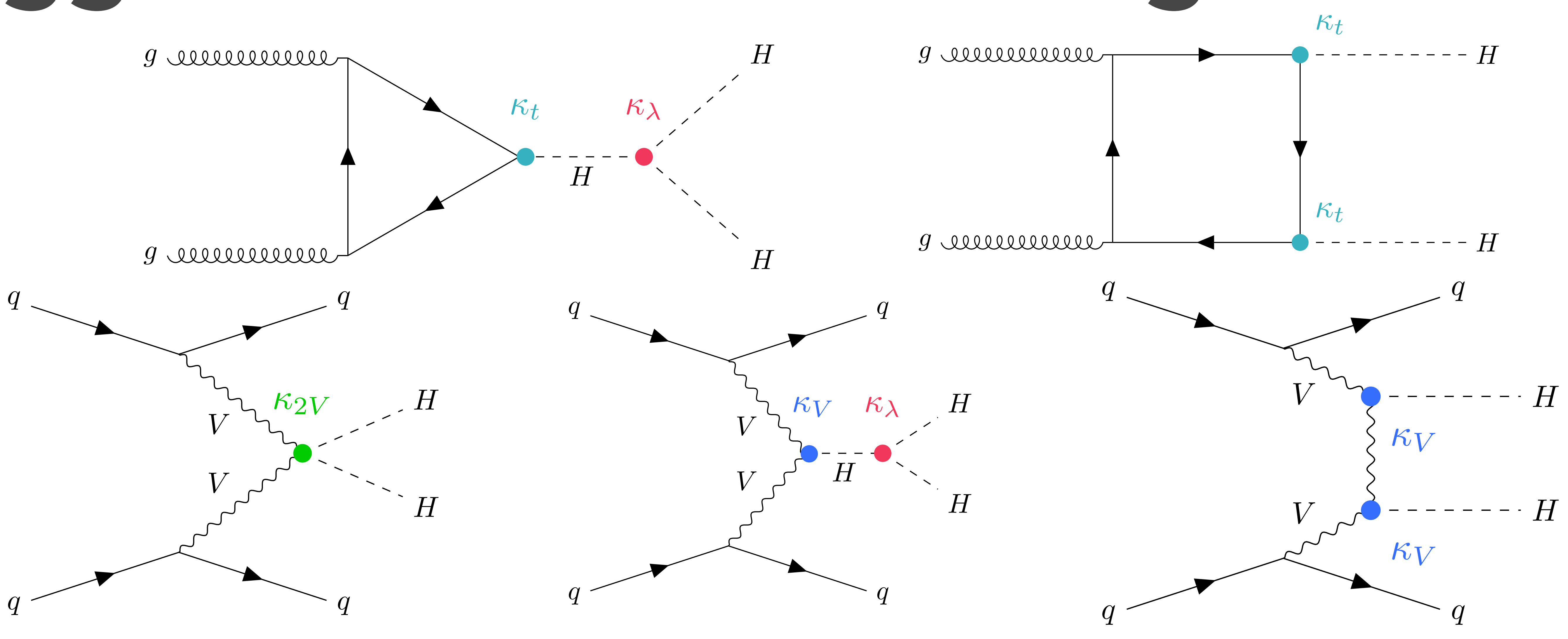

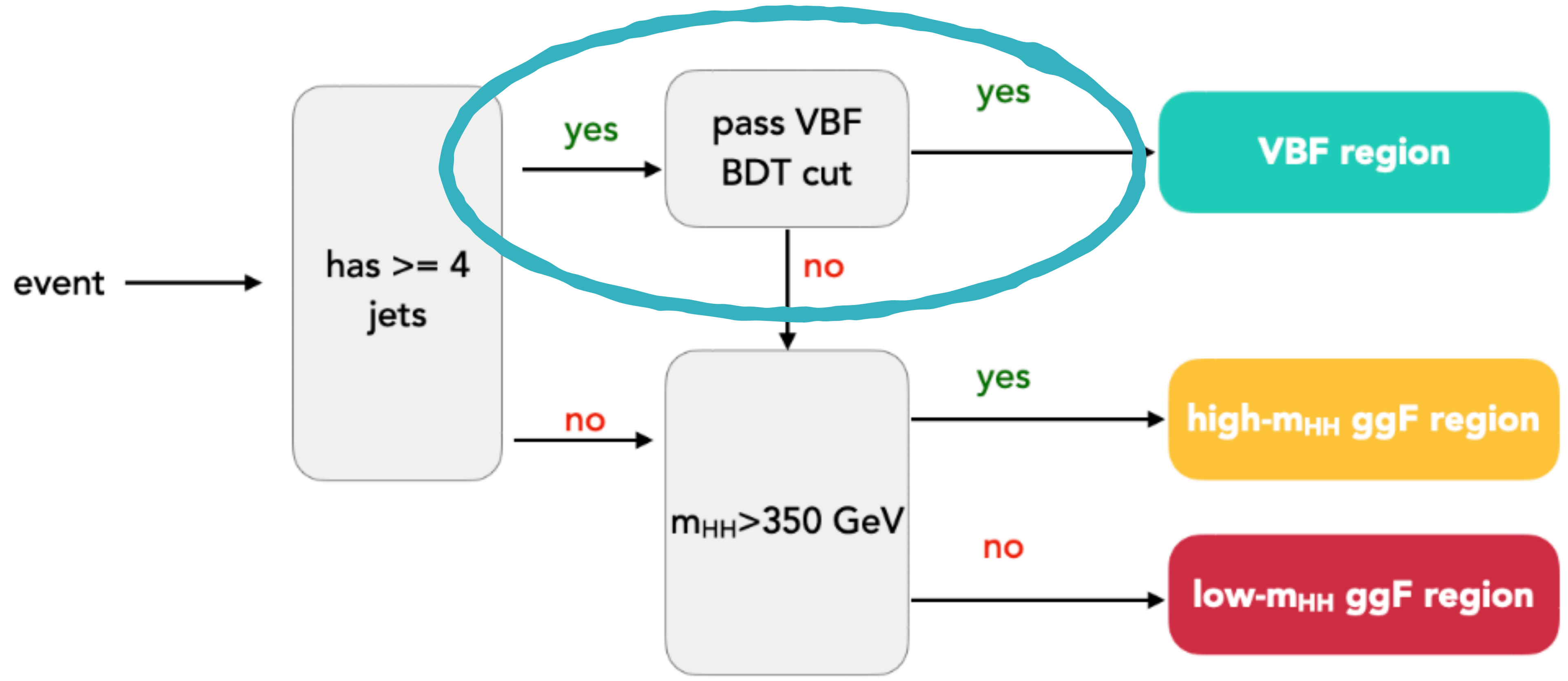

- Introduce dedicated VBF HH SR to improve κ_{2V} constraint and decorrelate signal production modes

- Train BDTs to separate ggF HH from VBF HH on events with at least 4 jets

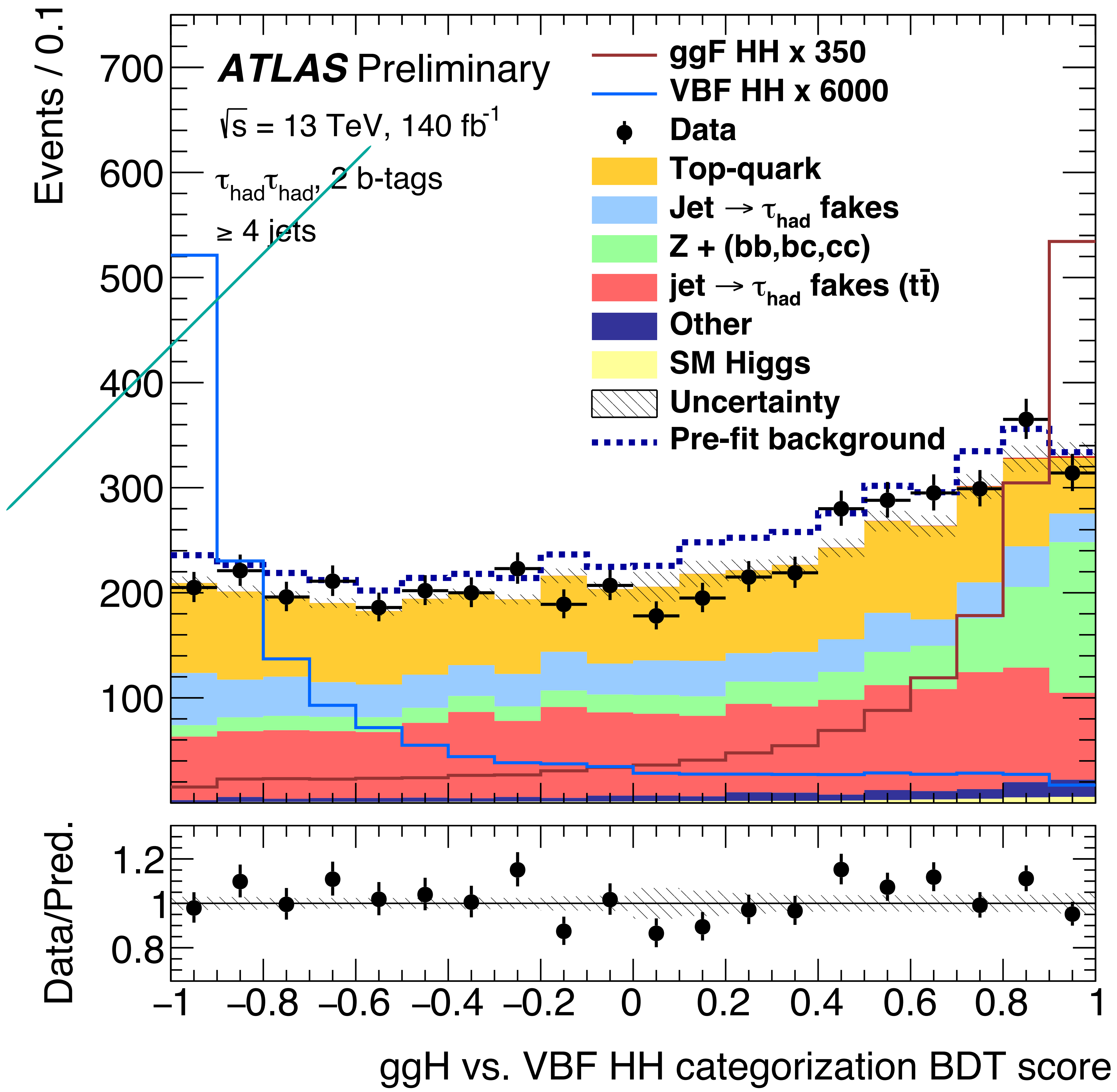

VBF category **ggF category**

Split in m_{HH}

- Further categorisation of ggF-like events with a cut at $m_{HH} = 350$ GeV
- Improve sensitivity to high κ_λ values which are more enhanced at low m_{HH}
- Signal vs background BDTs trained separately for each category

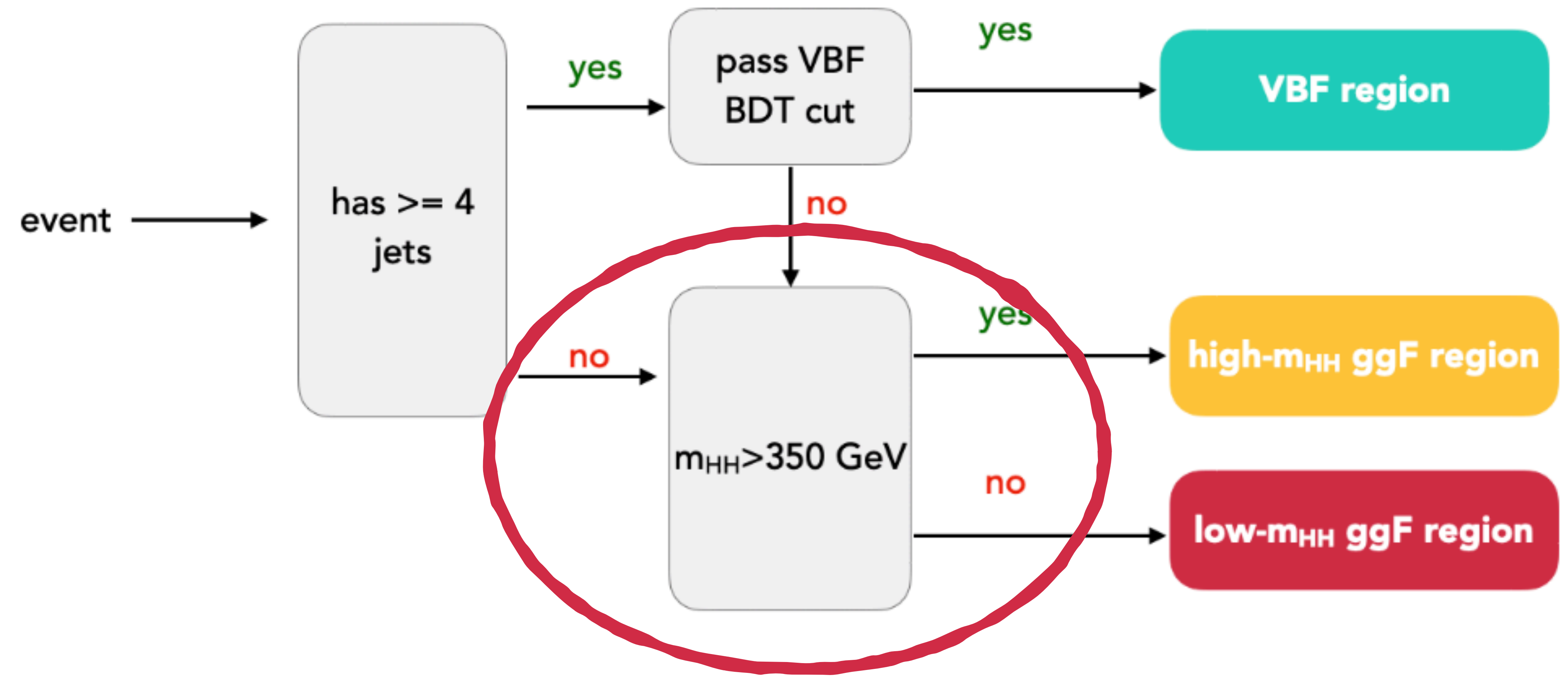

SM VBF HH vs all backgrounds

SM ggF HH vs all backgrounds

$\kappa_\lambda = 10$ ggF HH vs all backgrounds

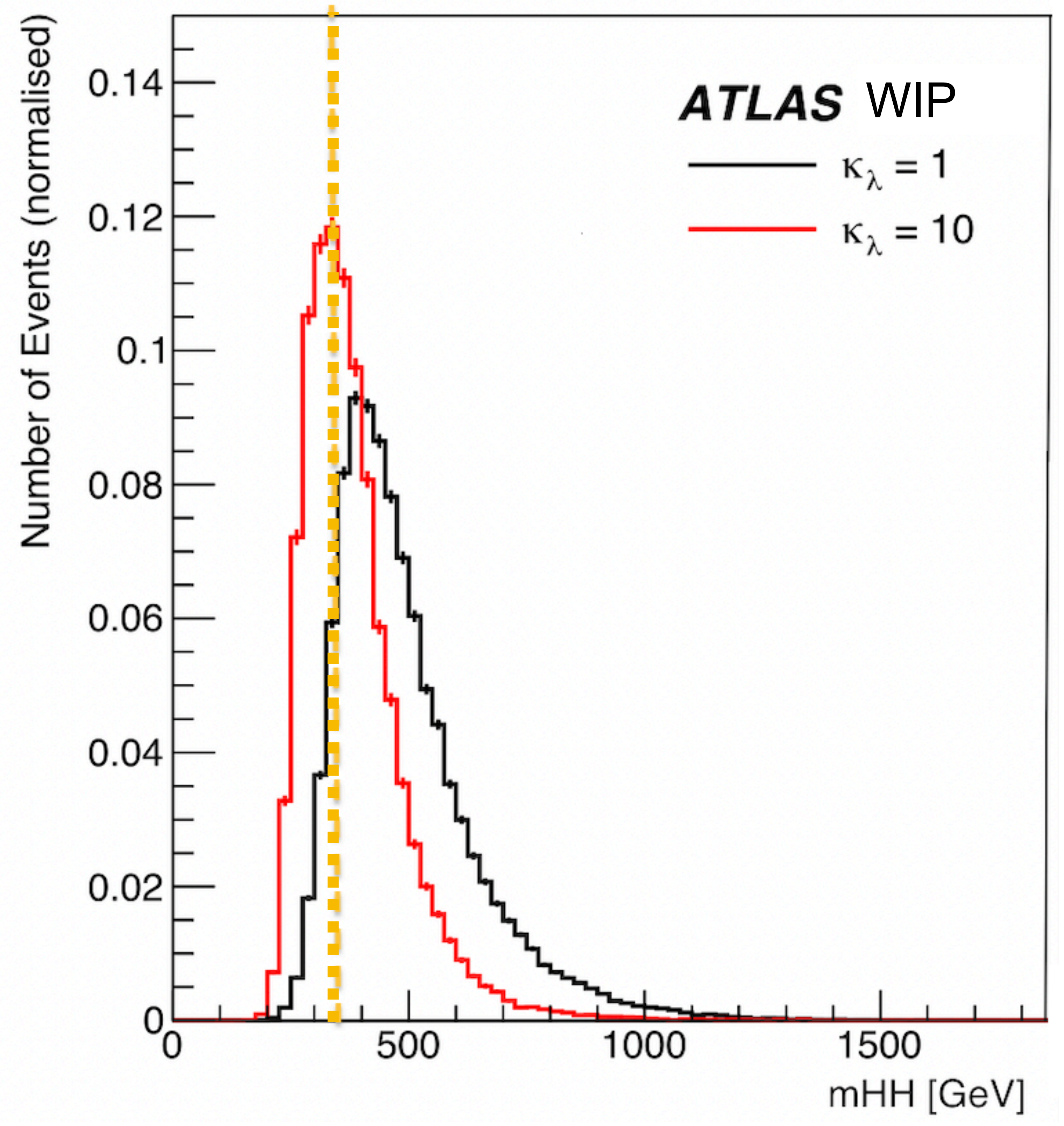

Post-fit plots

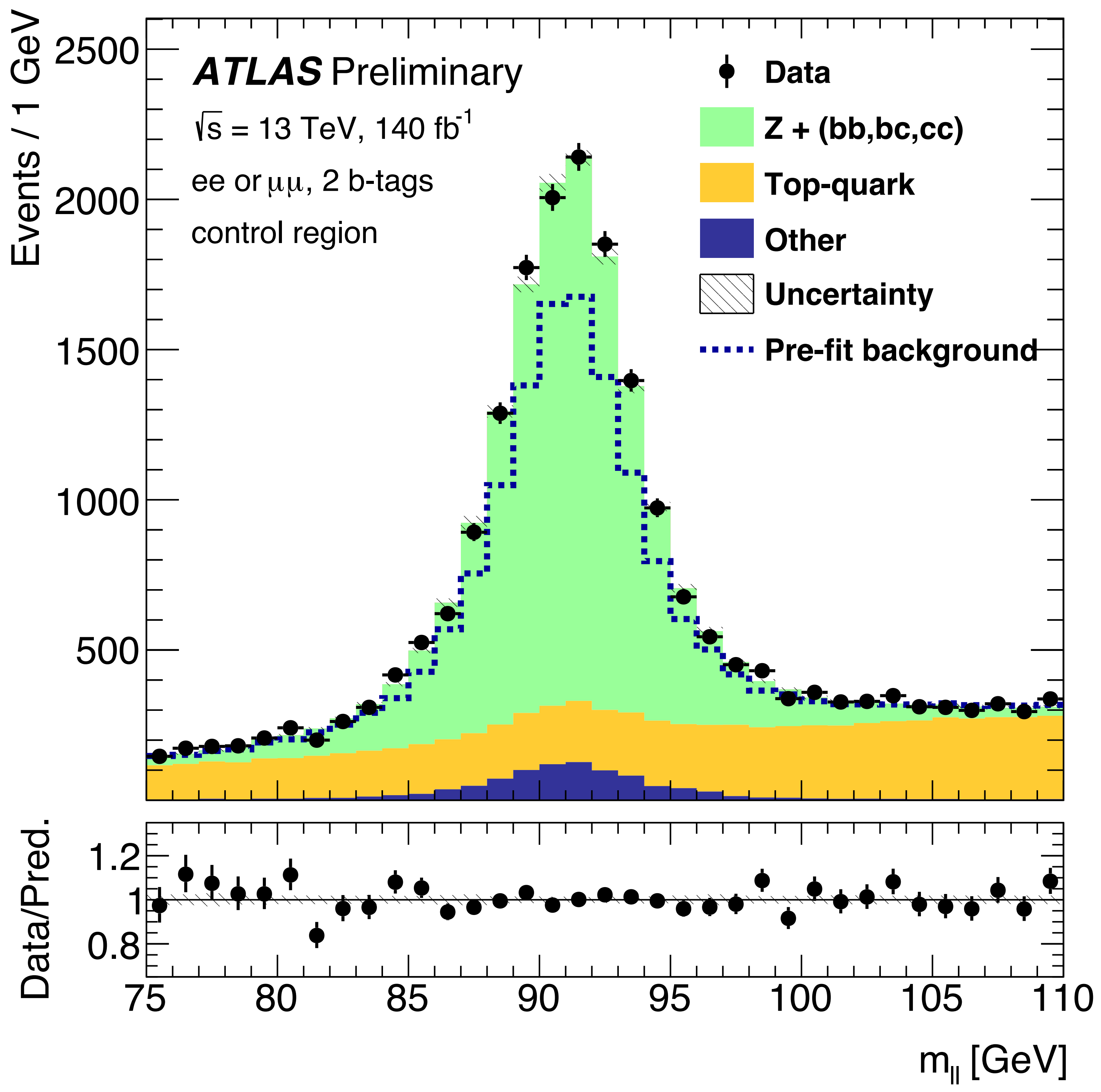

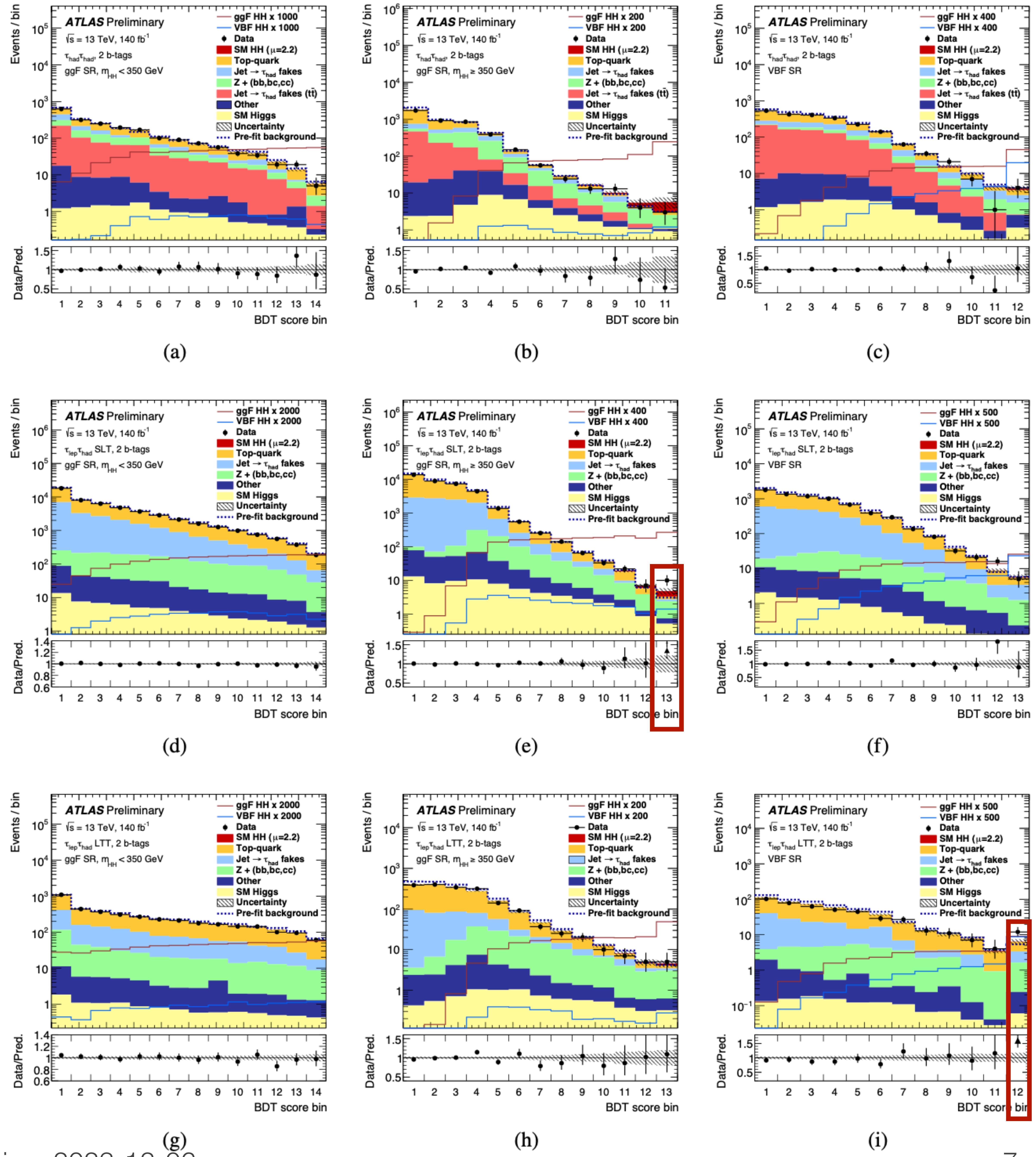

Signal strength limits

- No significant signal excess found
- Observed limit higher than expected due to 2.3σ fluctuation in $\tau_{lep}\tau_{had}$ SLT (high m_{HH} ggF category)
- Upper limits at 95% CL

$\mu_{HH} < 5.9$ (observed)

$\mu_{HH} < 3.1$ (expected) 20% improvement wrt previous result

Simultaneous fit of μ_{ggF} and μ_{VBF} thanks to new VBF SR

$\mu_{ggF} < 5.8\,(3.2)$ obs. (exp.)

$\mu_{VBF} < 91\,(71)$ obs. (exp.)

$$\mu_{ggF} = \frac{\sigma_{ggF}}{\sigma_{ggF}^{SM}}$$

$$\mu_{VBF} = \frac{\sigma_{VBF}}{\sigma_{VBF}^{SM}}$$

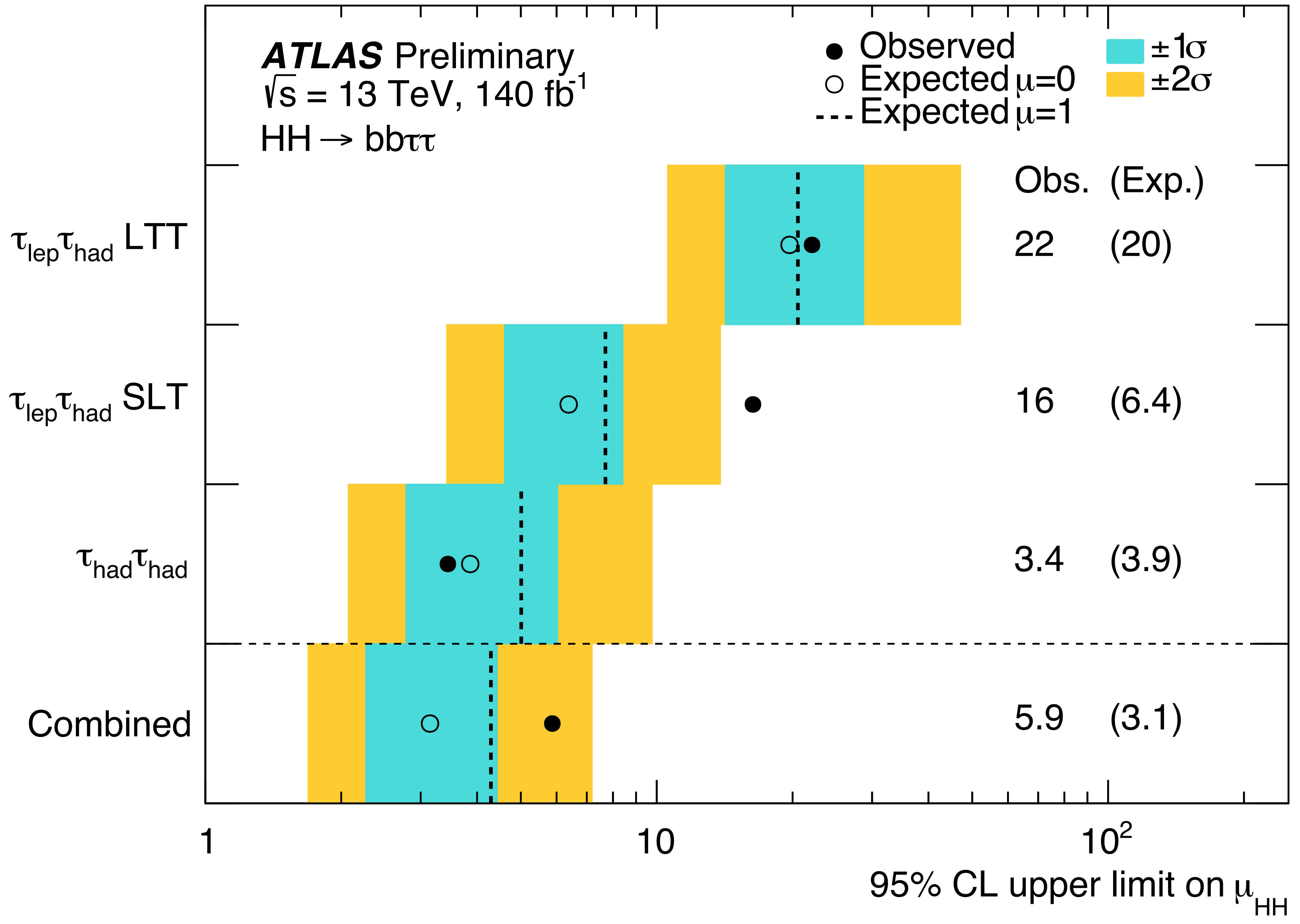

Constraints on coupling modifiers

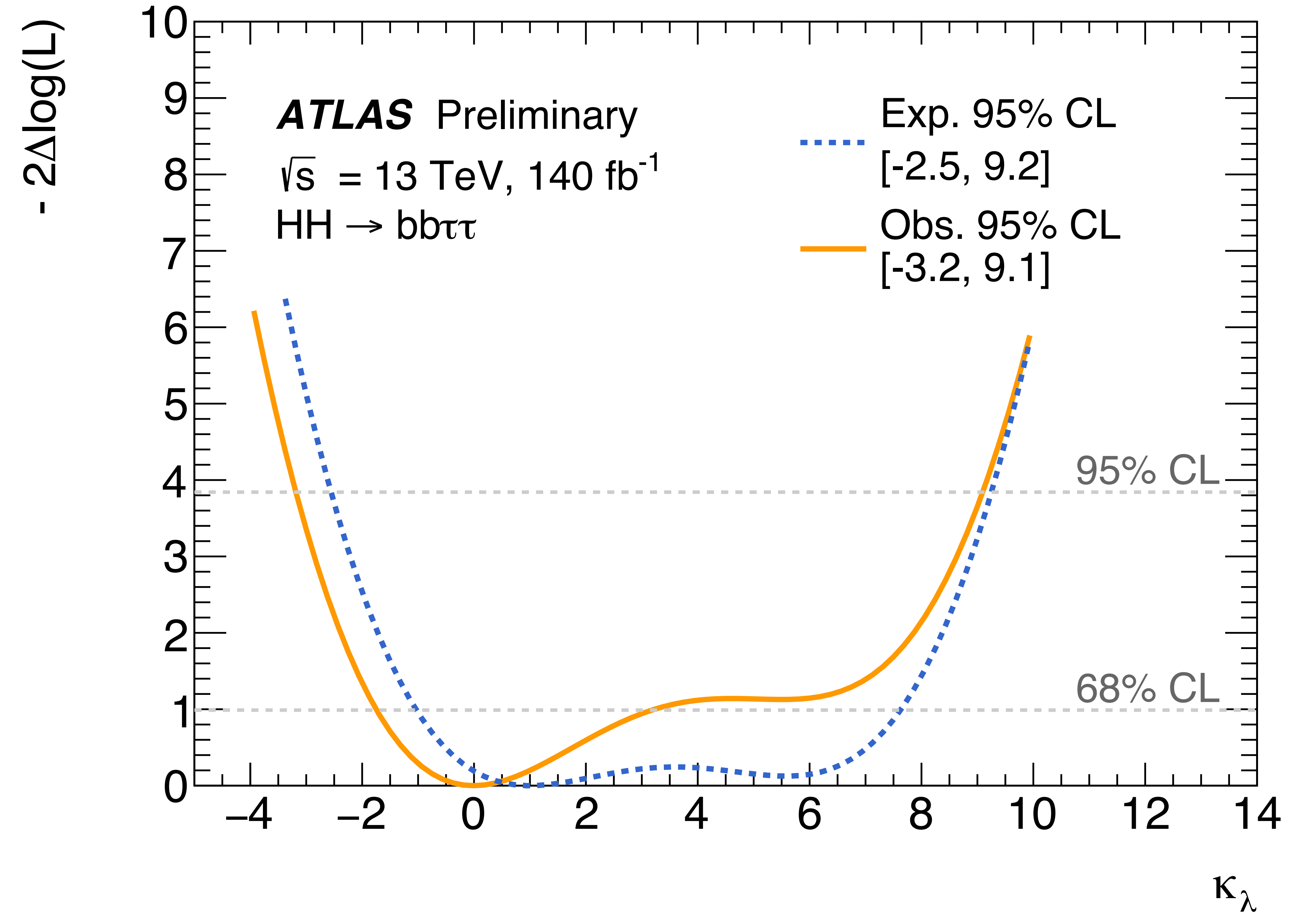

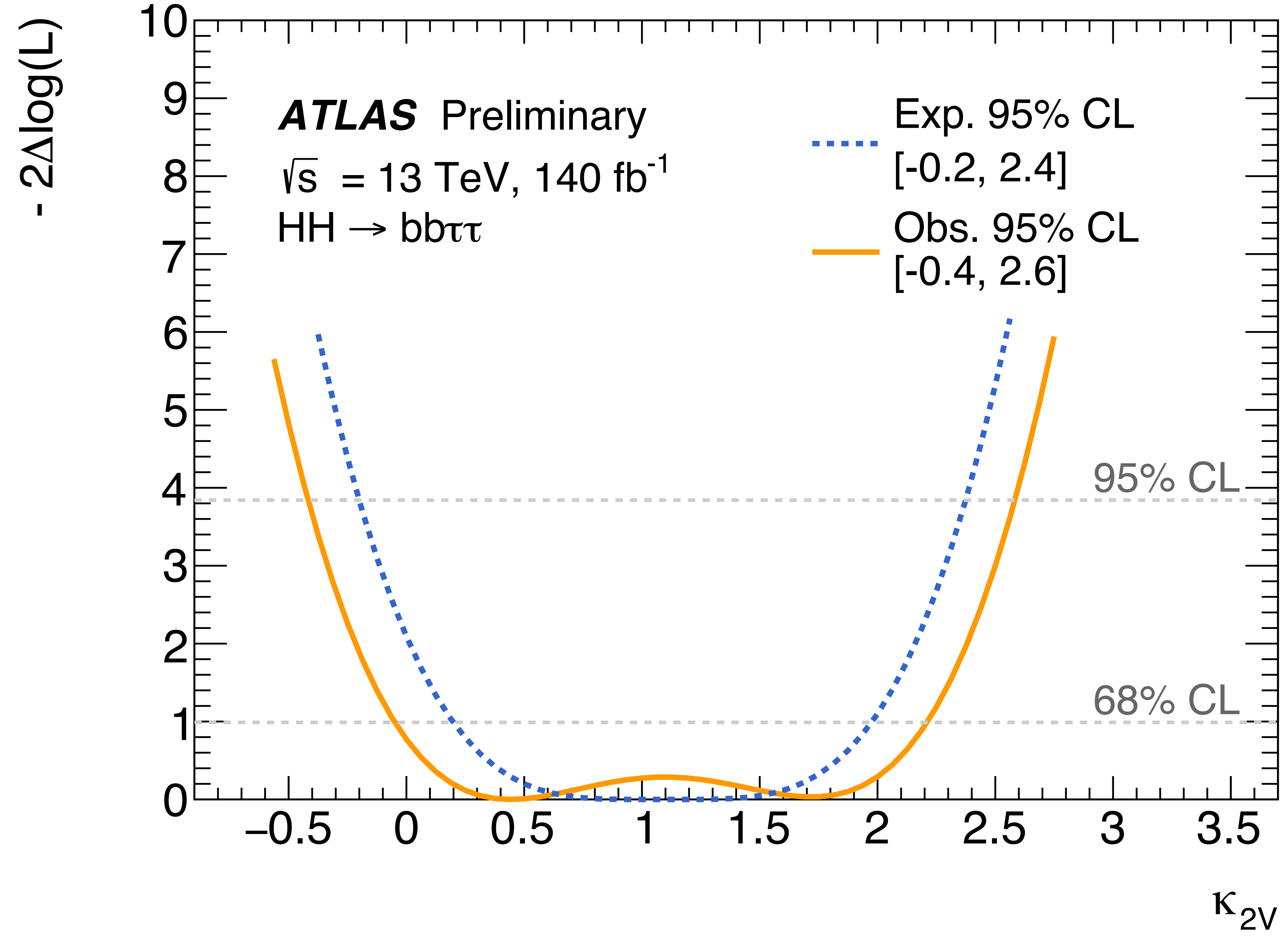

$\kappa_\lambda \in [-3.2, 9.1]$ (observed)

$\kappa_\lambda \in [-2.5, 9.2]$ (expected) 11% reduction in width

$\kappa_{2V} \in [-0.4, 2.6]$ (observed)

$\kappa_{2V} \in [-0.2, 2.4]$ (expected) 19% reduction in width

EFT interpretation: m_{HH} shape benchmarks

- Seven HEFT shape benchmarks proposed by theorists
- Cluster analysis used to group the various characteristic m_{HH} shapes

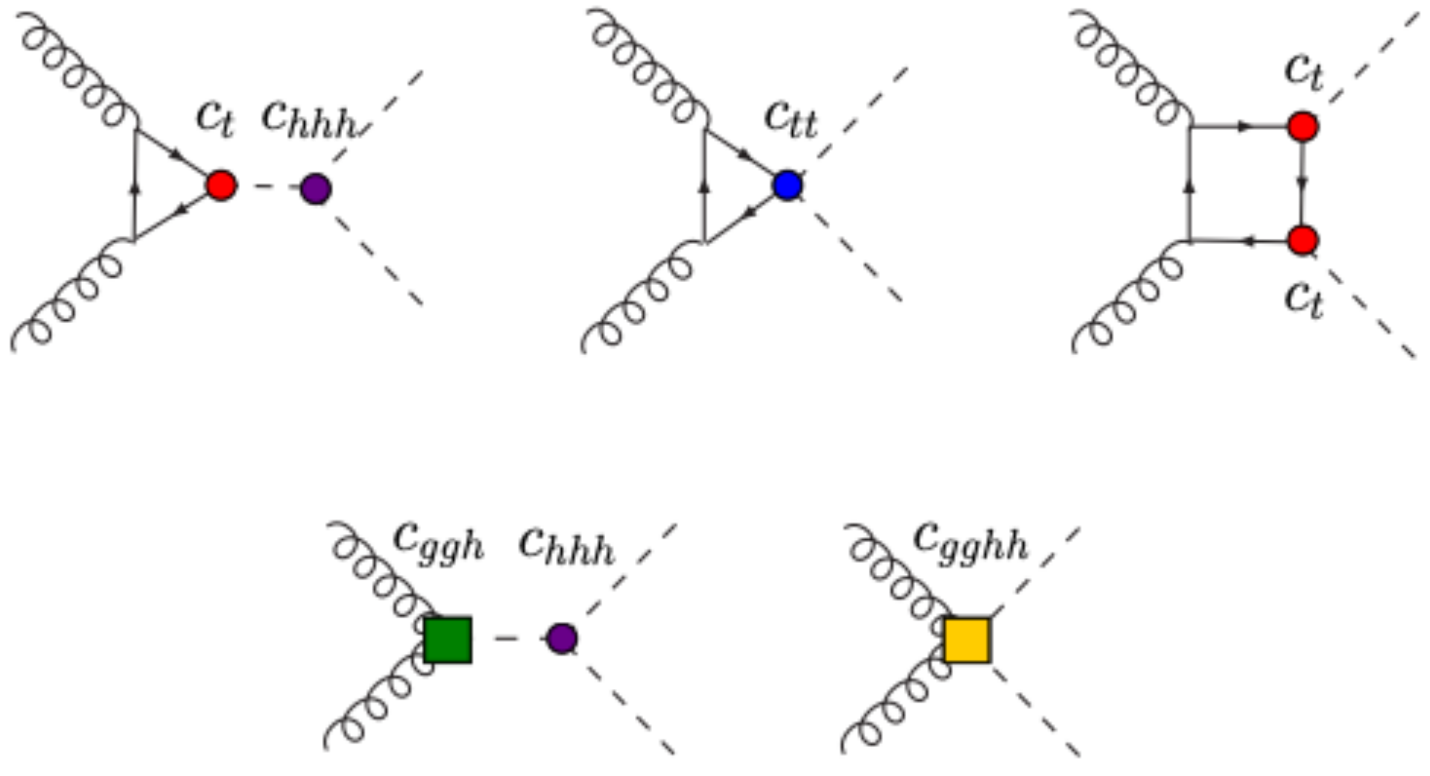

[arXiv:2304.01968]

benchmark (* = modified)	c_{hhh}	c_t	c_{tt}	c_{ggh}	c_{gghh}
SM	1	1	0	0	0
1*	5.11	1.10	0	0	0
2*	6.84	1.03	$\frac{1}{6}$	$-\frac{1}{3}$	0
3	2.21	1.05	$-\frac{1}{3}$	$\frac{1}{2}$	$\frac{1}{2}$
4*	2.79	0.90	$-\frac{1}{6}$	$-\frac{1}{3}$	$-\frac{1}{2}$
5	3.95	1.17	$-\frac{1}{3}$	$\frac{1}{6}$	$-\frac{1}{2}$
6*	−0.68	0.90	$-\frac{1}{6}$	$\frac{1}{2}$	0.25
7	−0.10	0.94	1	$\frac{1}{6}$	$-\frac{1}{6}$

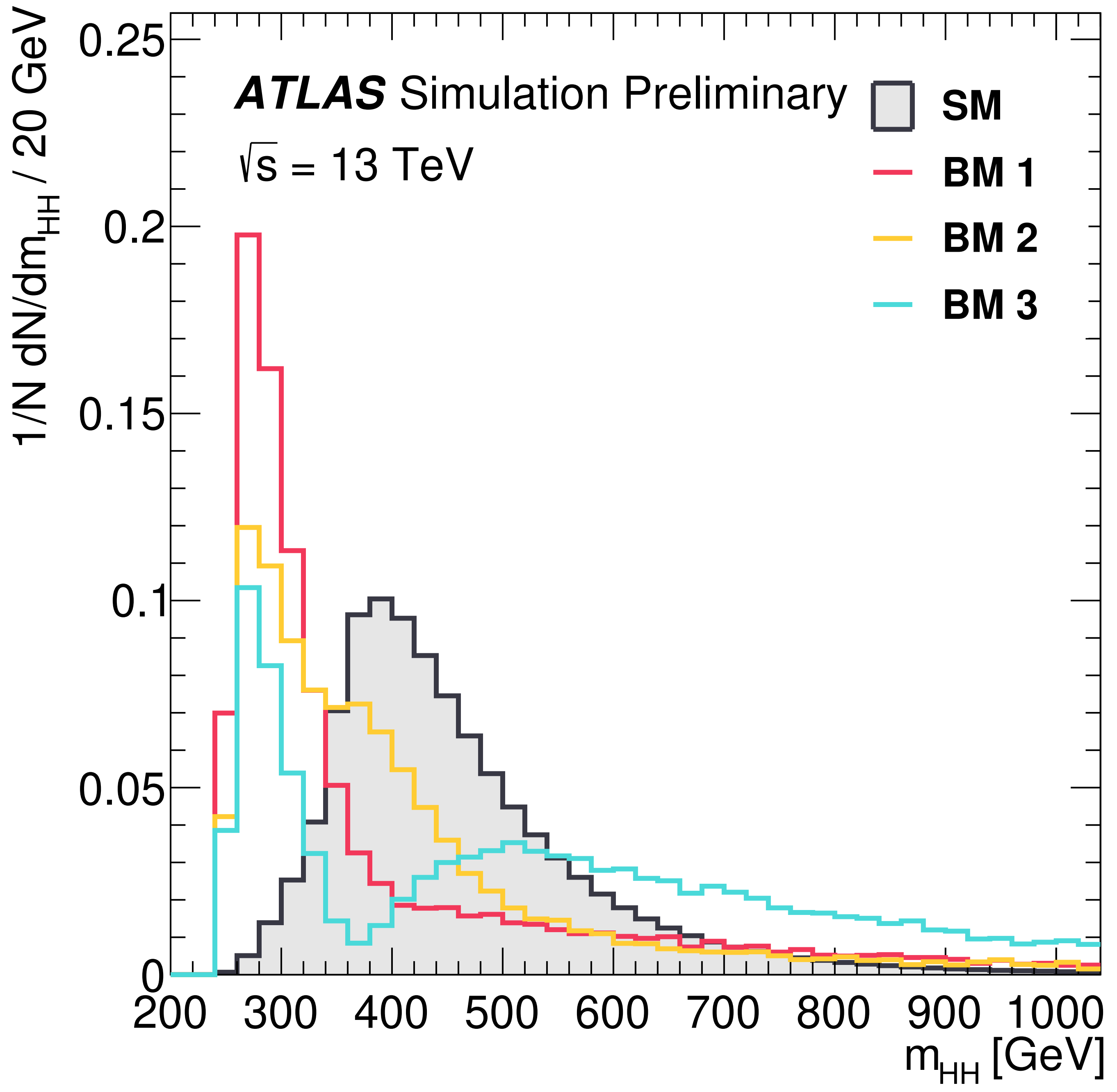

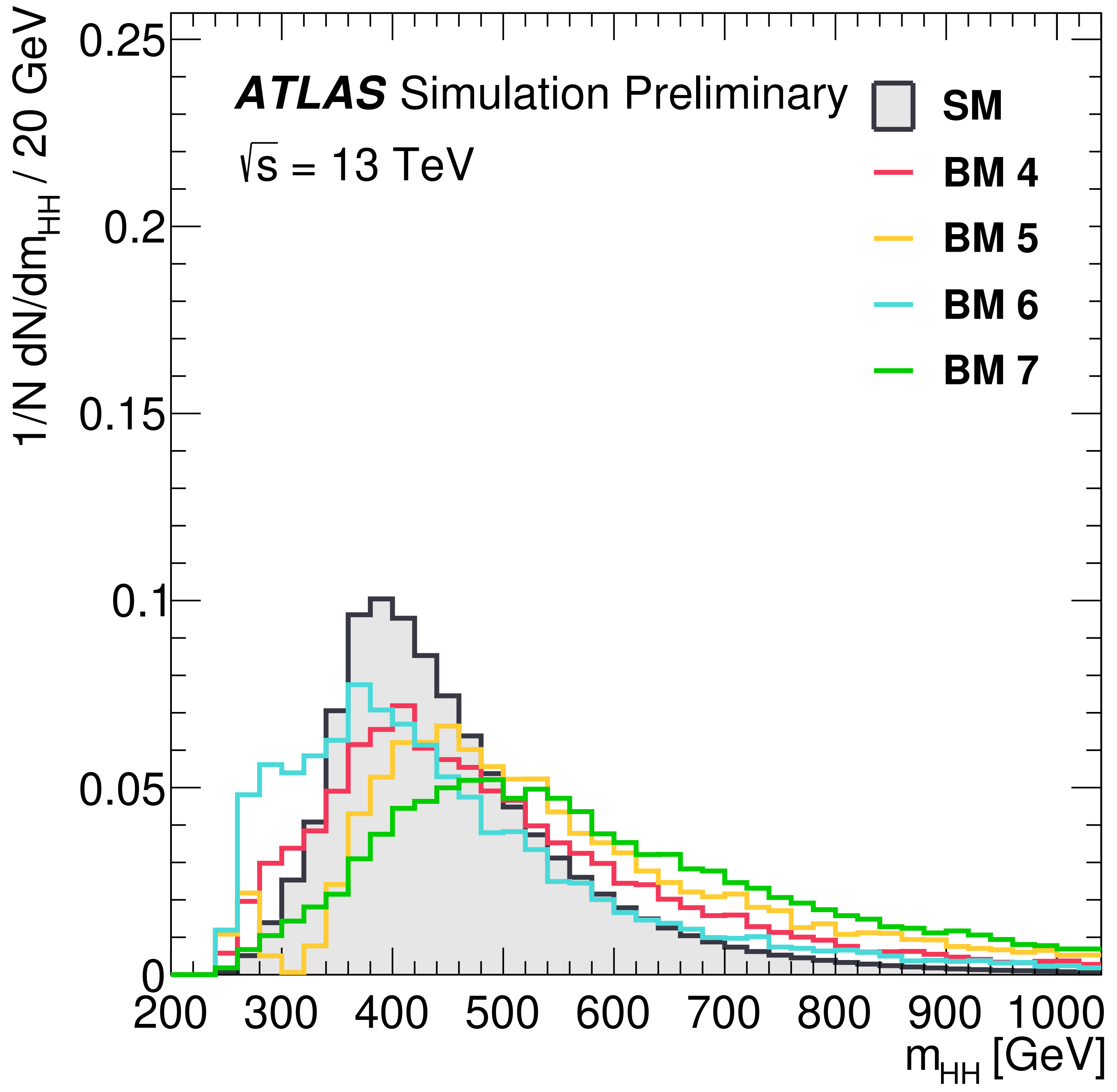

[ATL-PHYS-PUB-2022-019]

EFT interpretation: m_{HH} shape benchmarks

- Seven HEFT shape benchmarks proposed by theorists
- Cluster analysis used to group the various characteristic m_{HH} shapes

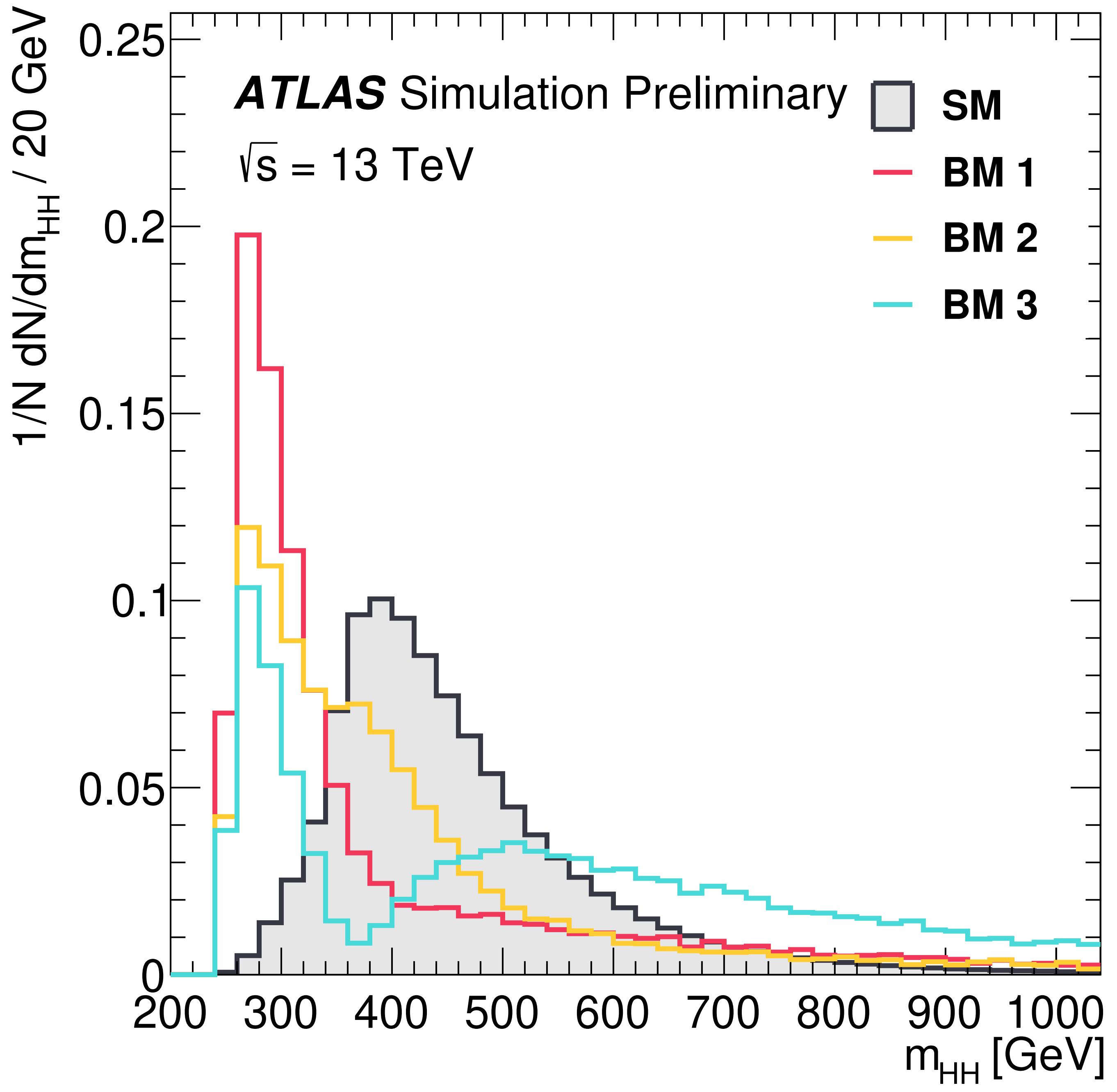

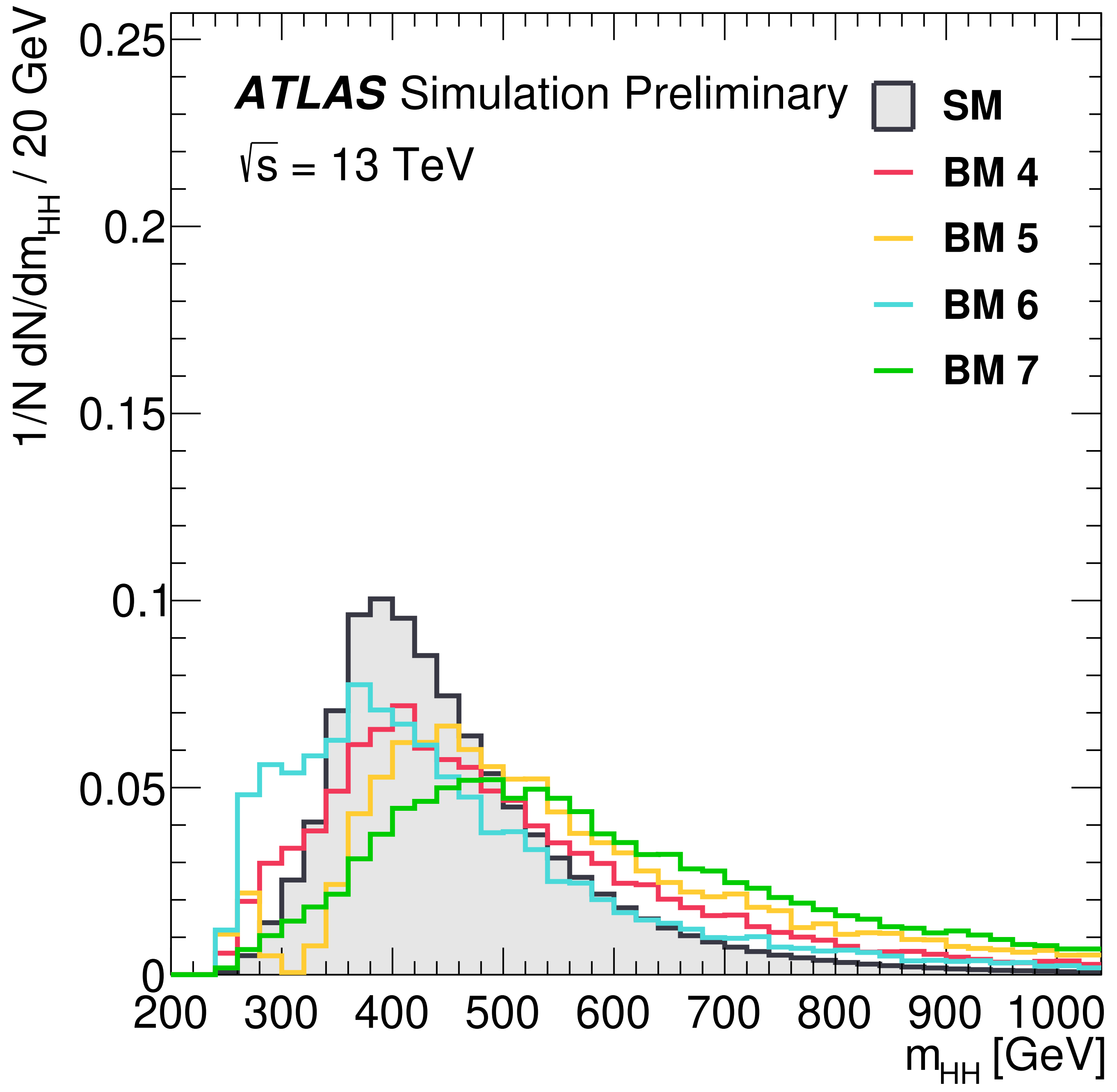

[ATL-PHYS-PUB-2022-019]

Upper limits on $\sigma_{ggF(HH)}$ for SM and 7 benchmarks

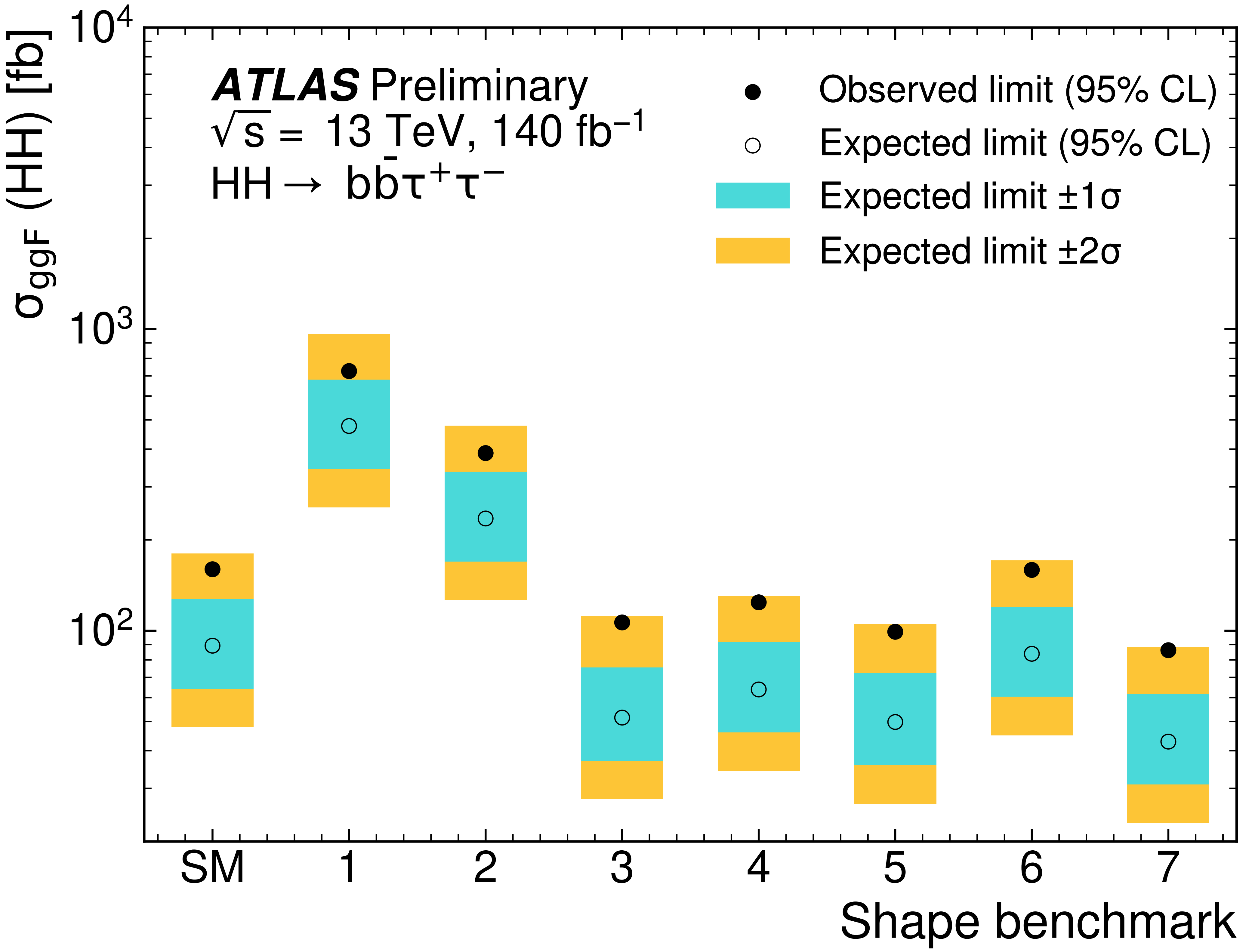

EFT interpretation (bonus)

- Wilson coefficients scans are also being currently prepared (to be included in the paper)
- Plan to set constraints on effective $ggHH$ and $ttHH$ couplings (HEFT framework)

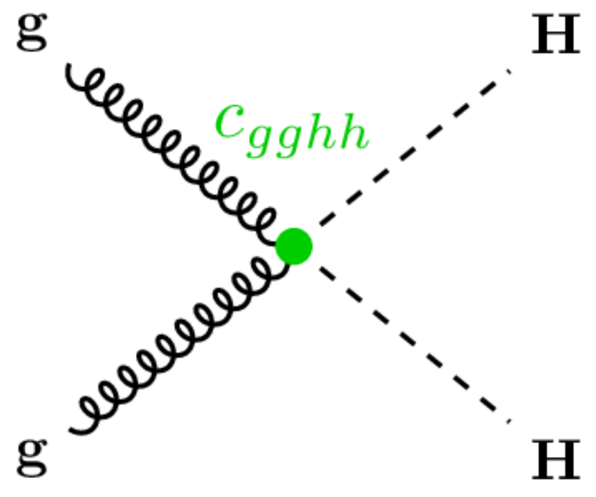

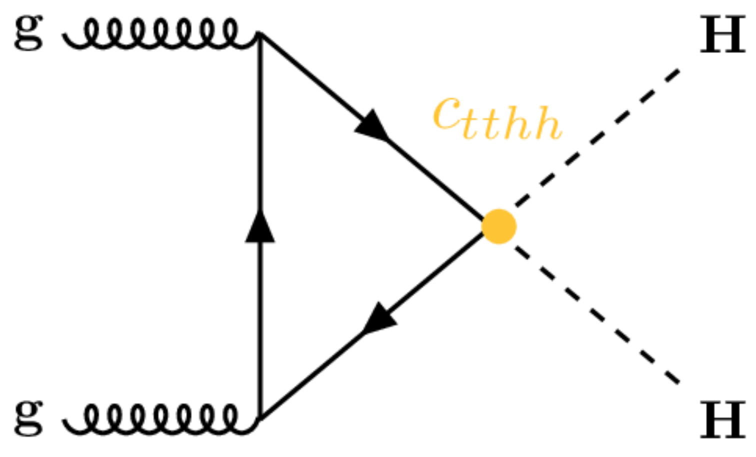

- Wilson coefficients c_H and $c_{H\Box}$

Wilson Coefficient	Operator
c_H	$(H^\dagger H)^3$
$c_{H\Box}$	$(H^\dagger H)\Box(H^\dagger H)$

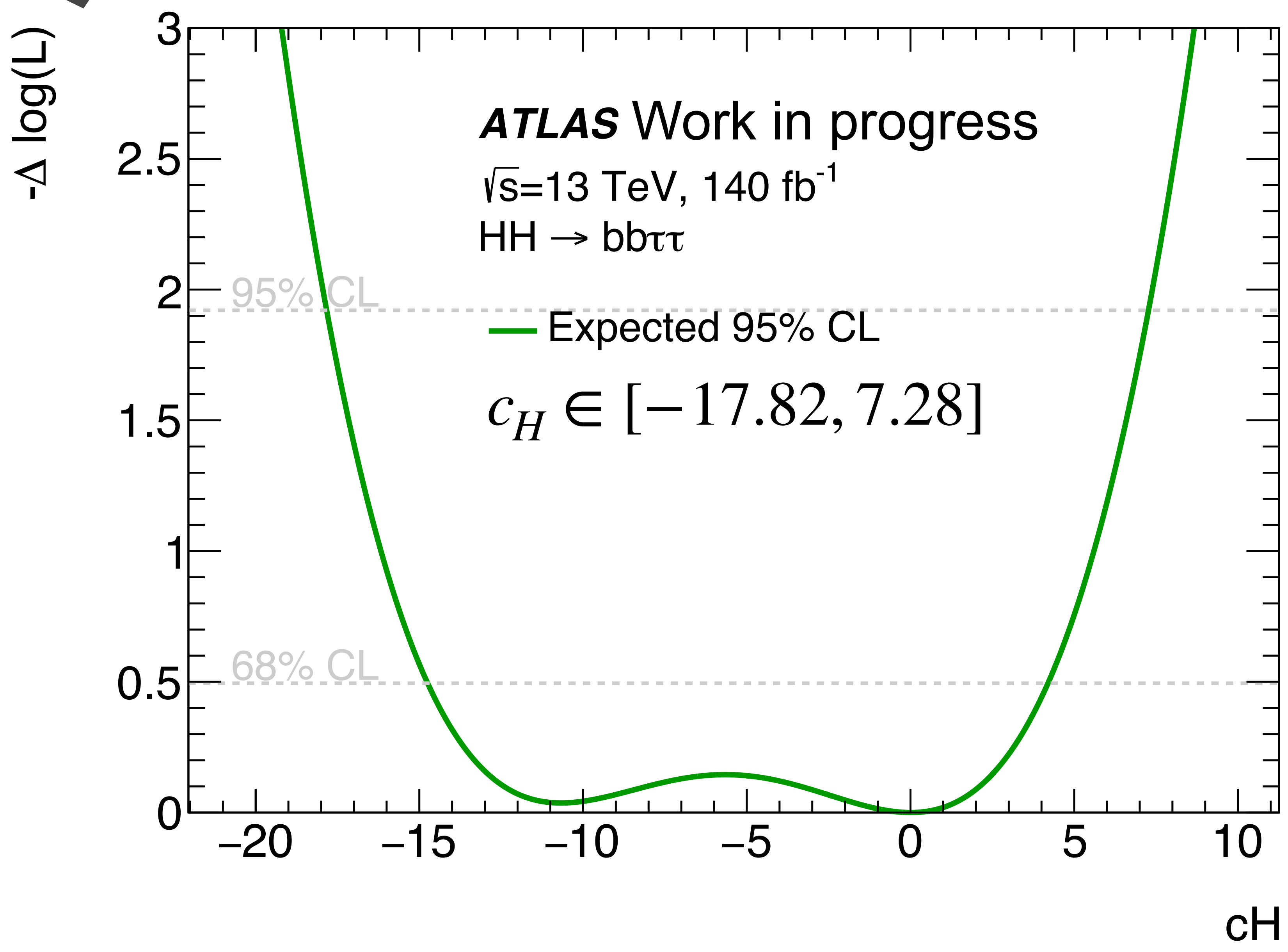

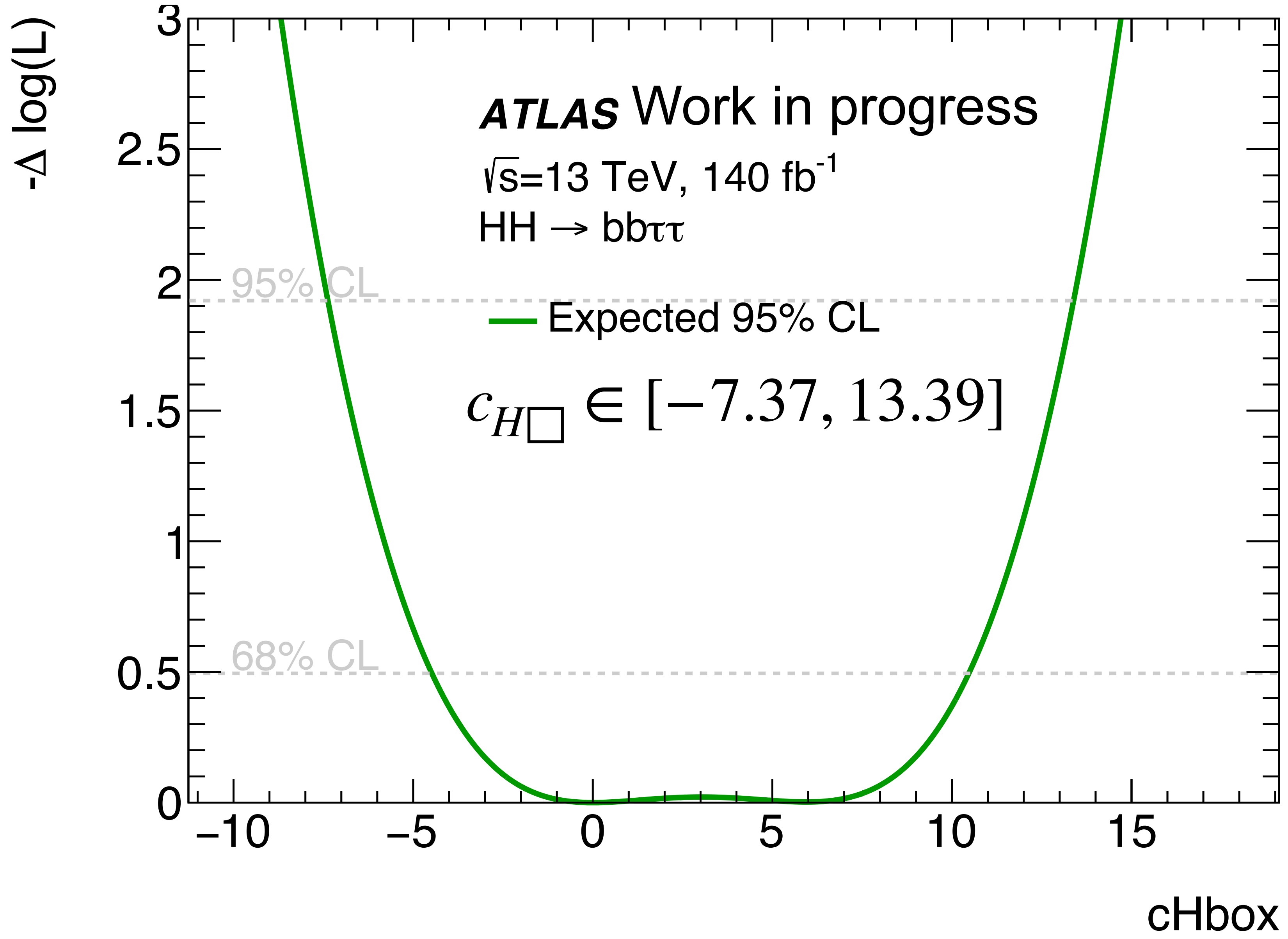

Run 3 plans

- Kick-off of Run 3 $HH \rightarrow bb\tau\tau$ a few weeks ago
- Work on (common) HH framework development
- Tentatively work on fake-tau background estimation
- The publication strategy is yet to be decided
  - $SH \rightarrow bb\tau\tau$ never published by ATLAS, so a public result with Run 2 + partial Run 3 datasets likely
  - Non-resonant $HH \rightarrow bb\tau\tau$: wait or not for 2024 data for a public result?
- Collaboration with theorists
  - Towards simplified models of compositeness and SUSY in HH (not specific to $bb\tau\tau$)

Back-up

Event selection flowchart

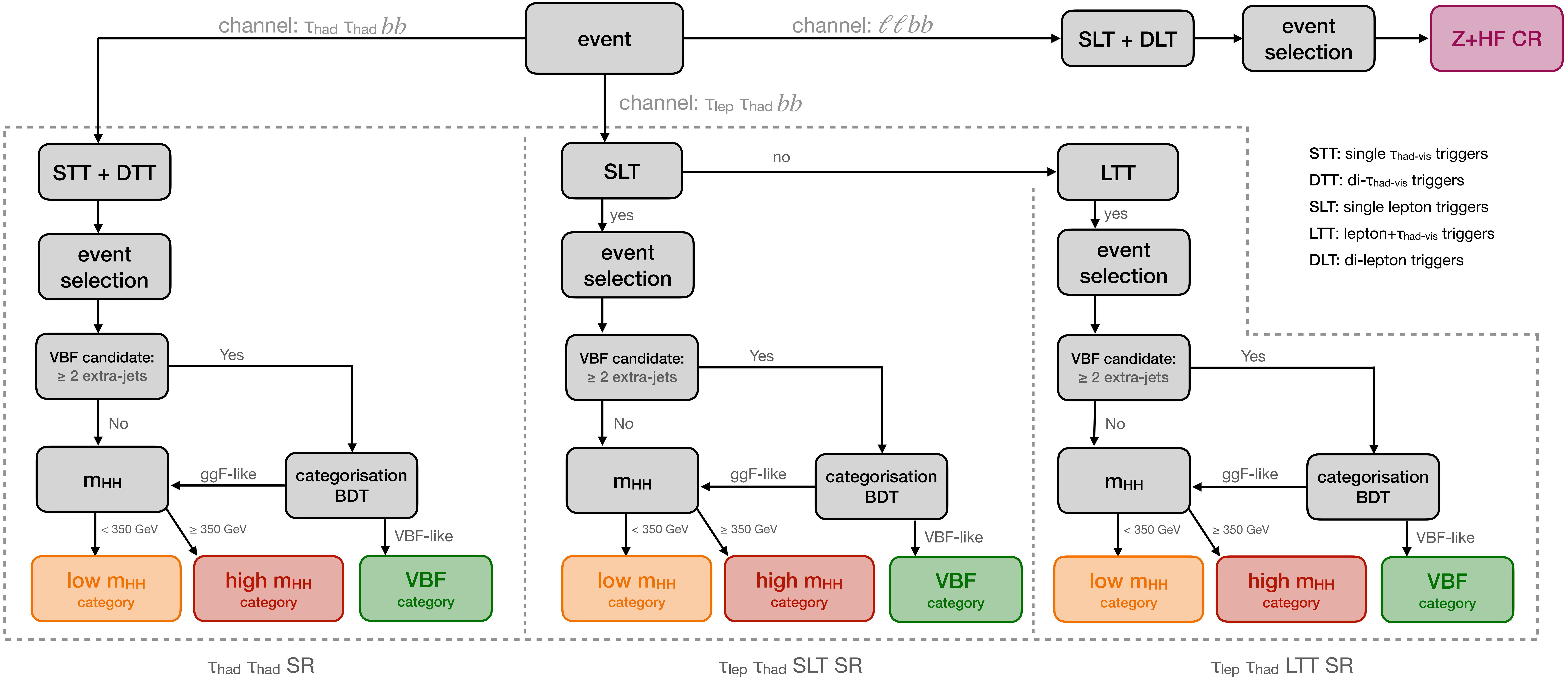

Differential cross-section

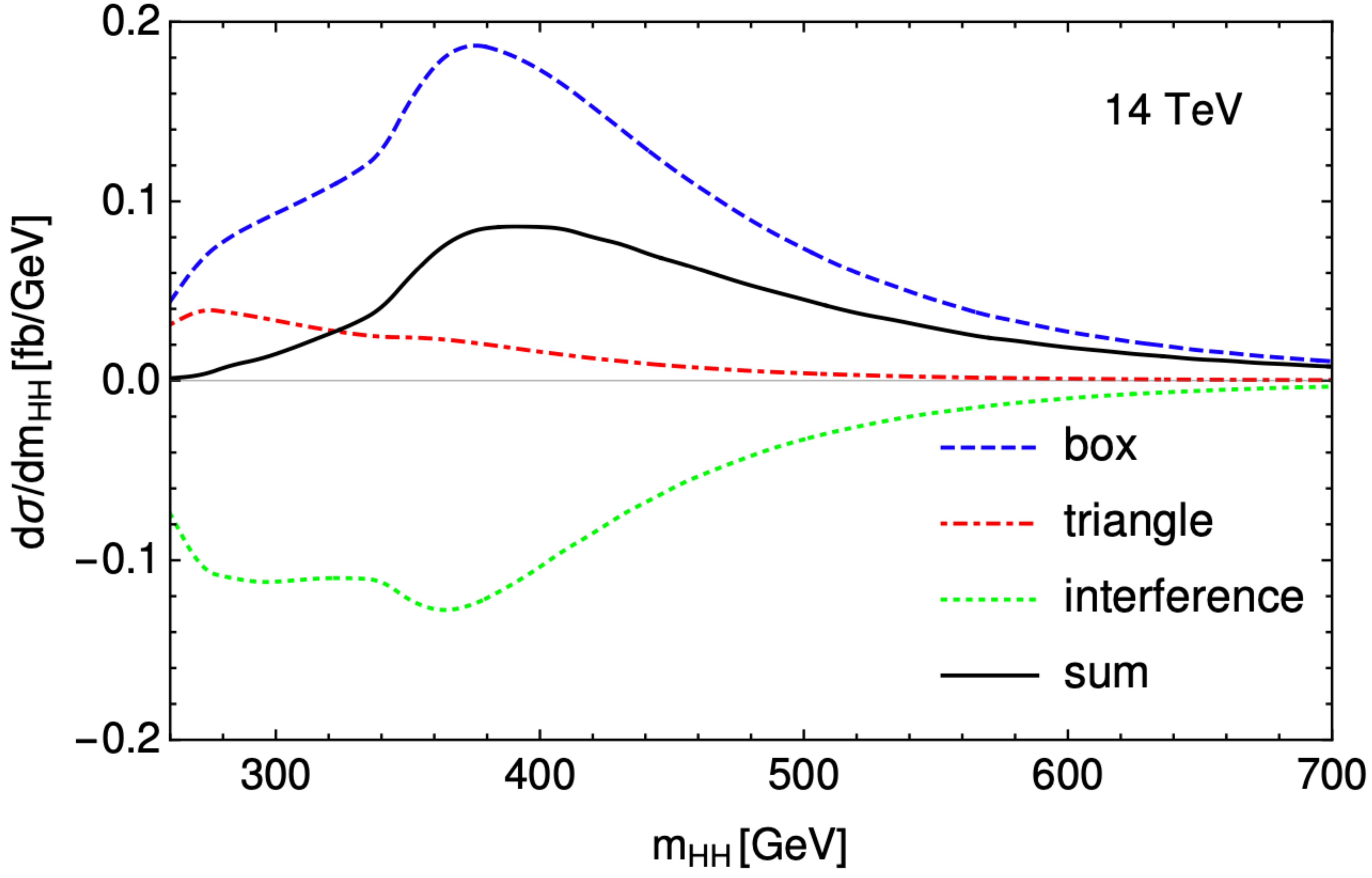

NLL scans per channel

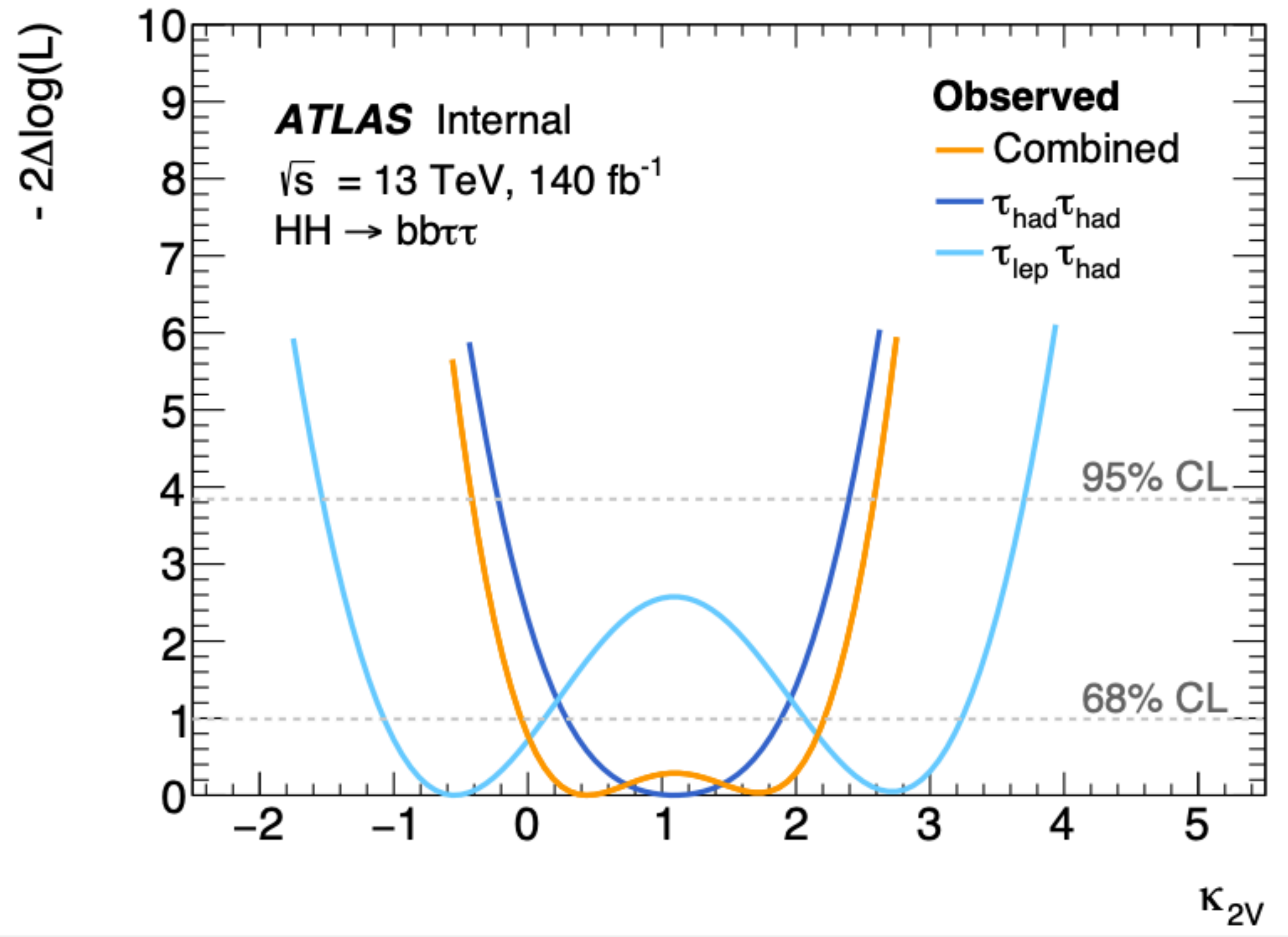

Deficit in hadhad, minimum at ~SM, smallest possible xsec
(SM predicts the lowest VBF yield)

Excess in lephad, best fit k2v values away from 1
(two k2v values that predict the same VBF yield)

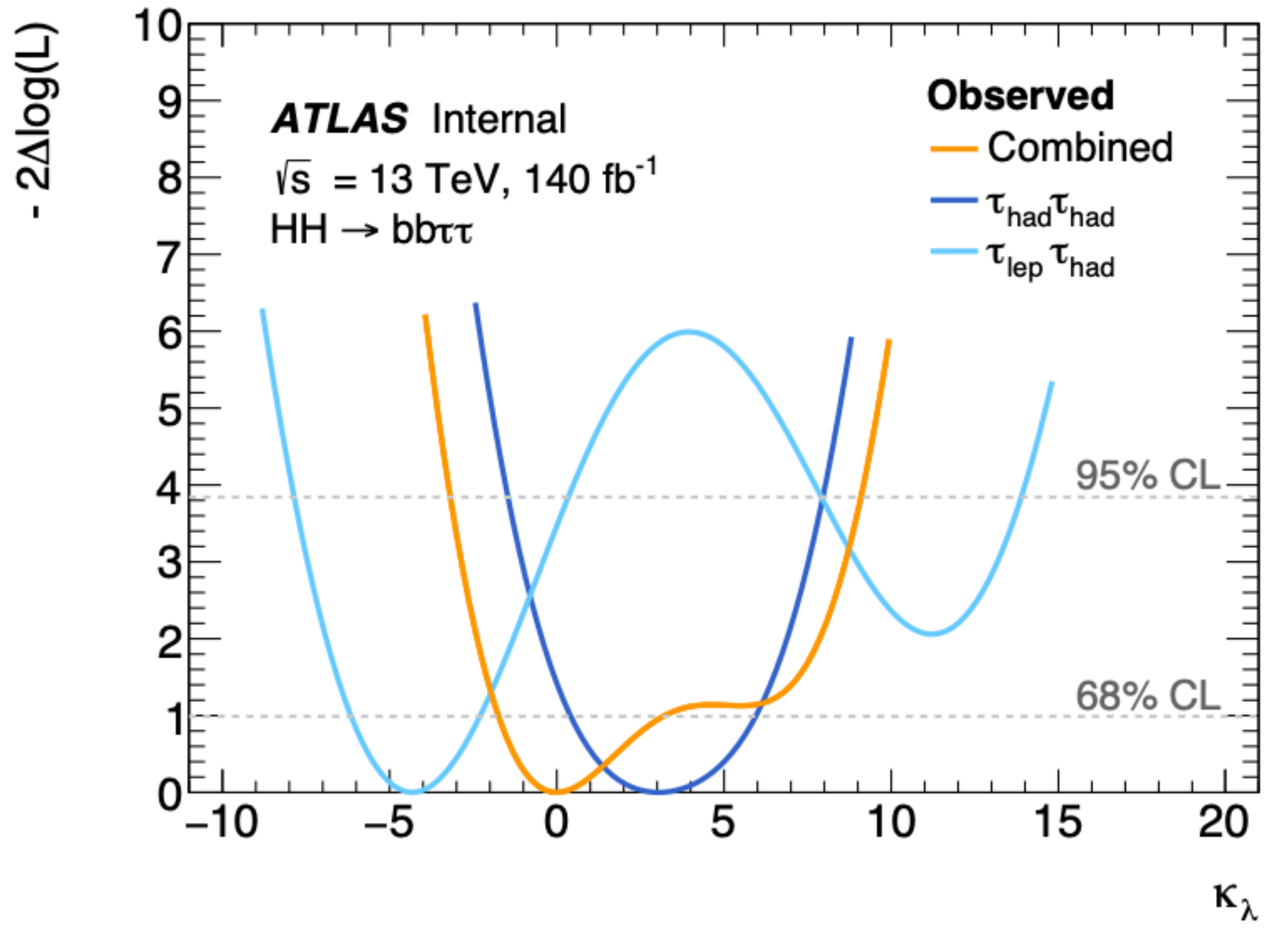

Deficit in hadhad, minimum at ~kl=2, where the yield is lowest

Here we can distinguish the two minima thanks to the ggF mHH categories.

EFT frameworks

SMEFT

- Canonical counting, expansion in $1/\Lambda$

$$\mathscr{L}_{\text{SMEFT}} = \mathscr{L}_{\text{SM}} + \sum_{n,i} \frac{c_i^{(n)}}{\Lambda^{n-4}} \mathcal{O}_i^{(n)}$$

- SM symmetries and fields, traditional EWSB mechanism (Higgs field: $SU(2)_L$ doublet)

- More restrictive (correlated effective couplings - ggh (tth) vertex related to $gghh$ ($tthh$) one)

HEFT

- No power-counting like in SMEFT, more similar to chiral perturbation theory

$$\mathscr{L}_{d_\chi} = \mathscr{L}_{(d_\chi=2)} + \sum_{L=1}^{\infty} \sum_i \left(\frac{1}{16\pi^2}\right)^L c_i^{(L)} O_i^{(L)}$$

- Higgs field: EW singlet

- Much more general (independent couplings)

HEFT in HH

- Five independent effective coupling coefficients, where $c_{hhh} = \kappa_\lambda$ and $c_{tth} = \kappa_t$

$$\mathscr{L}_{\mathrm{HEFT}} \supset -m_t \left(c_{tth}\frac{h}{v} + c_{tthh}\frac{h^2}{v^2} \right) \bar{t}t - c_{hhh}\frac{m_h^2}{2v}h^3 + \frac{\alpha_s}{8\pi}\left(c_{ggh}\frac{h}{v} + c_{gghh}\frac{h^2}{v^2} \right) G^a_{\mu\nu}G^{a,\mu\nu}$$

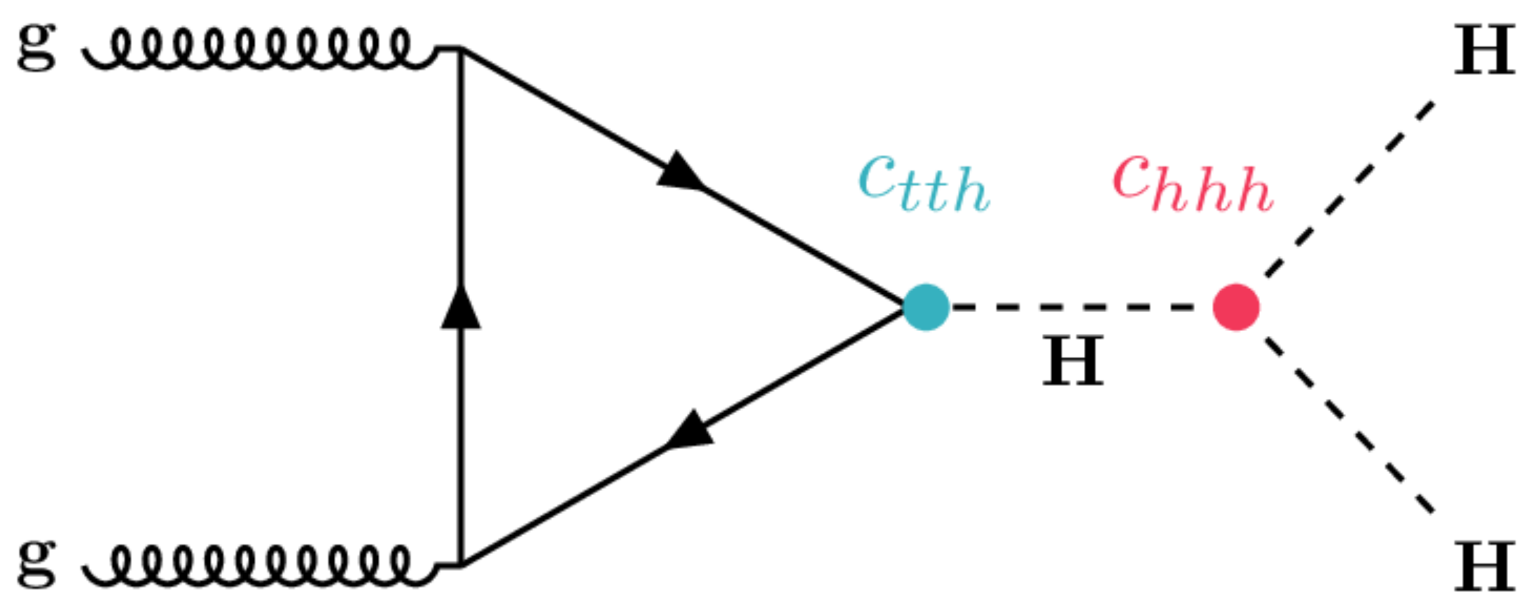

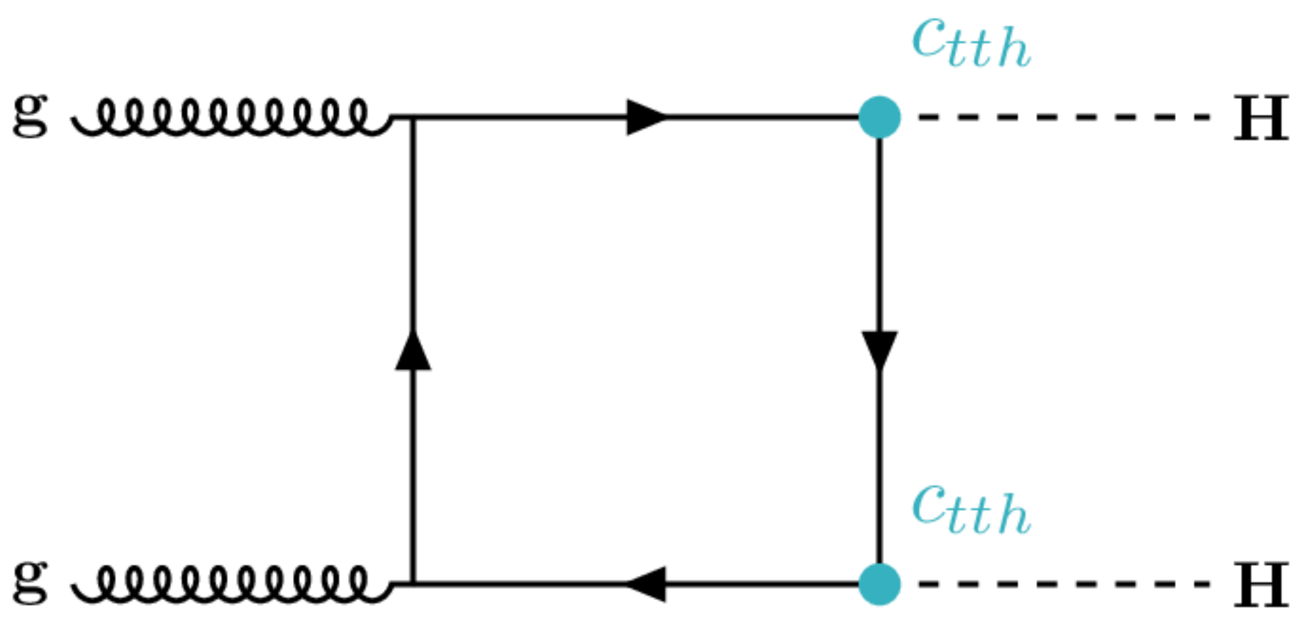

SM

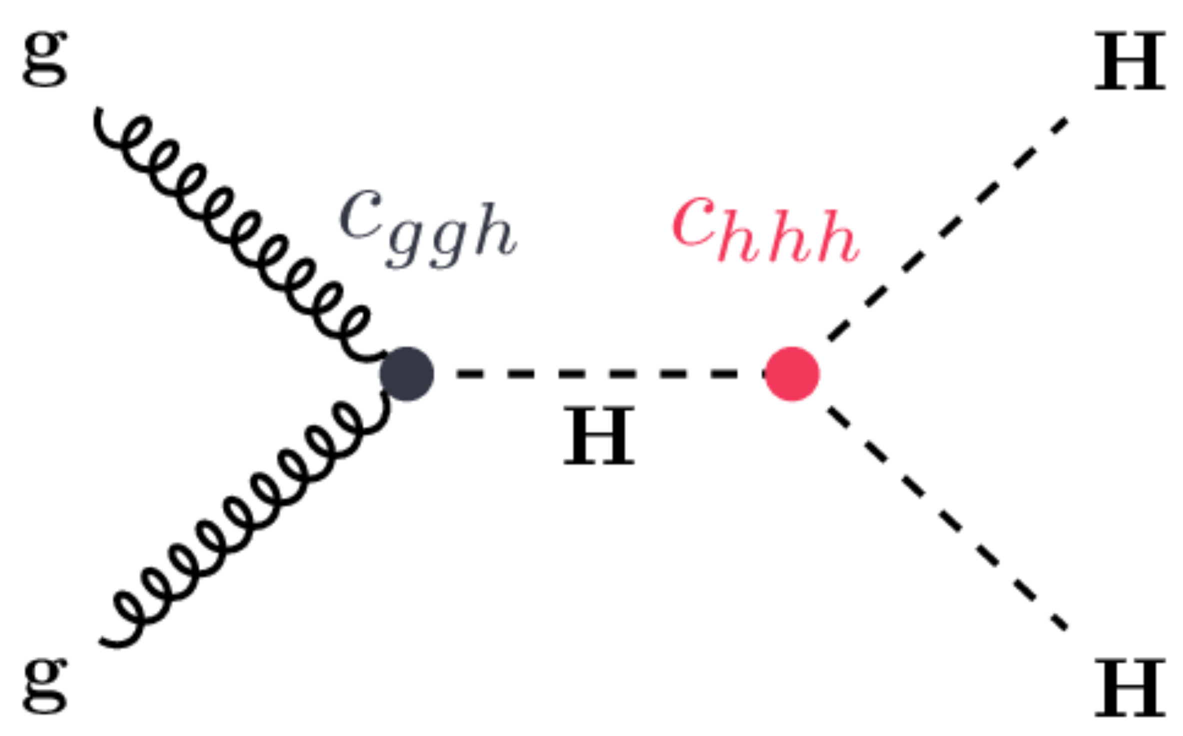

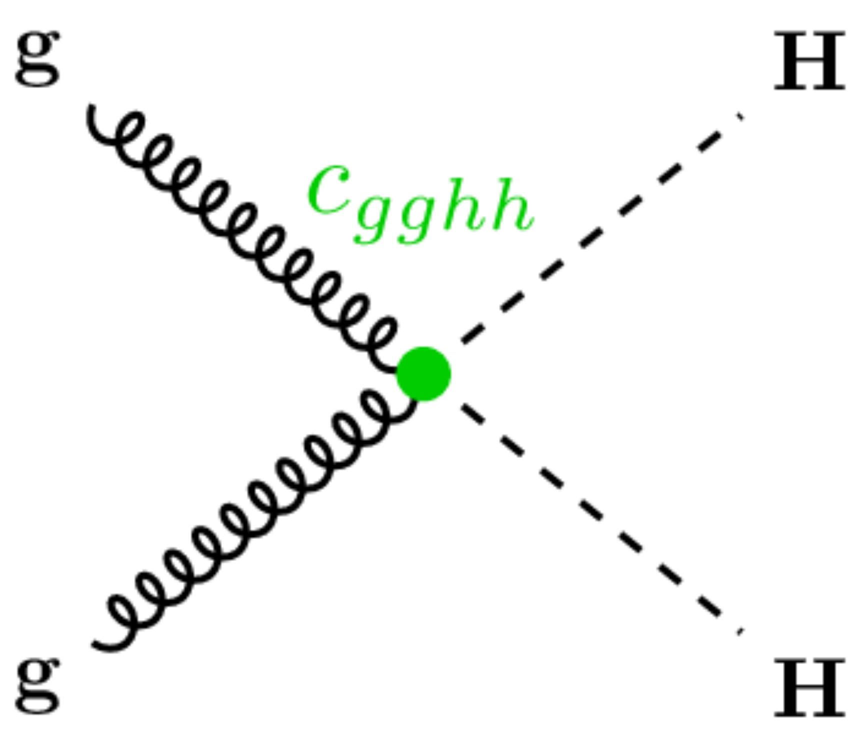

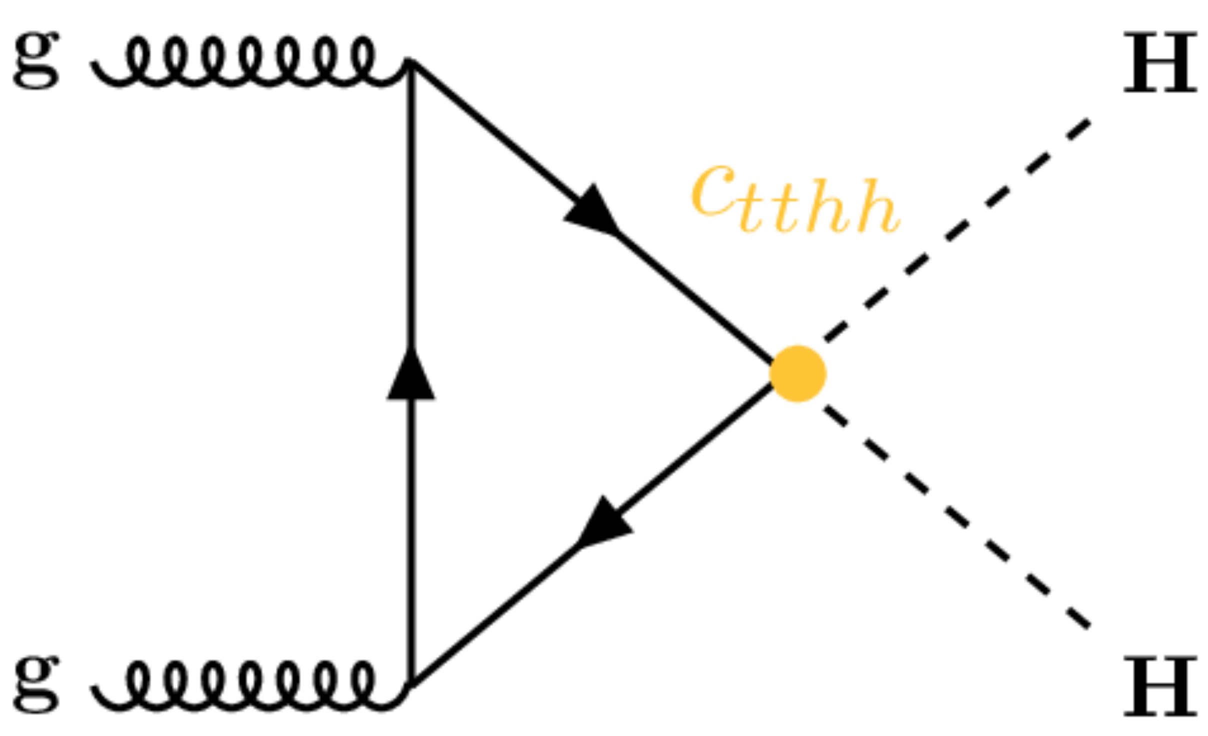

BSM

SMEFT in HH

- Wilson coefficients in the Warsaw basis: c_H, $c_{H\Box}$, c_{tH}, c_{HG} and c_{tG}

- In SM, all of them are zero

Not included in the HH EFT interpretations because it's constrained by other measurements

$$\mathcal{L}_{\text{SMEFT}} \supset \frac{C_{H\Box}}{\Lambda^2}(\phi^\dagger\phi)\Box(\phi^\dagger\phi) + \frac{C_{HD}}{\Lambda^2}(\phi^\dagger D_\mu\phi)^*(\phi^\dagger D^\mu\phi) + \frac{C_H}{\Lambda^2}(\phi^\dagger\phi)^3$$
$$+(\frac{C_{tH}}{\Lambda^2}\phi^\dagger\phi\bar{q}_L\tilde{\phi}\,t_R + \text{h.c.}) + \frac{C_{HG}}{\Lambda^2}\phi^\dagger\phi G^a_{\mu\nu}G^{\mu\nu,a}$$
$$+\frac{C_{tG}}{\Lambda^2}(\bar{q}_L\sigma^{\mu\nu}T^a G^a_{\mu\nu}\tilde{\phi}\,t_R + \text{h.c.})$$

- Contrary to HEFT, the only operator that gets **unique sensitivity** from HH is c_H

- Operators affecting $gghh$ and $tthh$ vertices are better constrained by **single Higgs production**